immune response by interacting with $CD4^+$ T or B cells and in organization of the follicular structure.

In HIV infection, human FDCs can capture and retain infectious HIV particles in a stable manner on their cell surfaces for several months or even years via Fc receptors or other molecules (22–25). Unlike conventional DCs, FDCs are not themselves infected with HIV despite expression of chemokine receptors and DC-SIGN (24). Furthermore, active HIV infection is largely confined to sites surrounding the FDCs (24), suggesting that this microenvironment is highly conducive to infection with this virus. FDCs have also been shown to transmit signals to the GC microenvironment which also appears to increase HIV infection and replication (24, 25). Our previous study showed that FDCs stimulated virus production in MOLT-4 T cells preexposed to HIV-1(23). Very recently, Thacker et al. (26) also reported that FDCs contributed to virus replication in $CD4^+$ T cells infected with HIV-1 obtained from peripheral blood and GCs by increasing viral transcription mediated by TNF-α upon coculture. However, the role of FDCs in HIV-infected monocytes/macrophages is largely unknown.

We here report that FDCs can activate HIV-1 production in surrounding infected monocytes or macrophages via a cell-cell interaction with a clear mechanistic distinction from $CD4^+$ T cells reported by Thacker et al. (26). This enhancement in monocytic cells was found to be mediated mainly by an association between P-selectin on FDCs, acting as a ligand, and P-selectin glycoprotein ligand 1 (PSGL-1), the cognate receptor, on HIV-1-infected cells. Furthermore, we delineate the biological significance of the PSGL-1/spleen tyrosine kinase (Syk) pathway in the FDCs-mediated switch to induce HIV-1 replication. Our current findings thus shed new light on mechanisms involved in the HIV replication pathway that are mediated through intercellular communication and provide clues for the design of future novel therapeutic interventions against AIDS and related disorders.

Materials and Methods

Cell culture and reagents

Several FDC lines were established from fresh human palatine tonsils and maintained as described previously (23). Briefly, FDCs were isolated from fresh palatine tonsils surgically removed. Tonsils were cut into pieces in the thickness of 2–3 mm and then digested for 15 min at 37°C with collagenase (type I; Wako). Following rinsing with RPMI 1640 by centrifugation at 400 × *g* for 7 min, cells were filtered through at 70-μm nylon mesh and overlaid on a 1.25, 2.5, and 5% continuous BSA gradient at 1 × *g* for 2 h. The lowest fraction with a higher density fraction was resuspended and cultured in RPMI 1640 medium with 10% FCS. Cell clusters in the lowest fraction included cells positive for DRC-1, a specific maker of FDCs. One week after the culture, adherent spindle-shaped FDCs appeared from the cell clusters after having released lymphoid cells and spontaneously proliferated without additional cytokines or growth factors. The character of FDCs was checked with expression of FDCs makers such as CAN-42, S-100α, CD54, DC-SIGN, and CXCR4 on its surface. After culturing along more than 2 wk, FDCs were stocked in −80°C before use. PBMCs were separated from three healthy donors in accordance with the guidelines of the ethics committee of Tokyo Medical and Dental University. PBMCs were cultured in RPMI 1640 containing 10% FBS at 37°C in 5% CO_2. Primary monocytes were obtained from three healthy donors with Rosette Sep (StemCell Technologies) according to the manufacturer's instructions. Primary macrophages were differentiated from monocytes by culturing in RPMI 1640 containing 10% AB serum (Sigma-Aldrich) and 20 ng/ml M-CSF (R&D Systems) for 7 days. HIV-1 chronically infected monocytic cell line U1 cells (27) were cultured in RPMI 1640 supplemented with 10% FBS (Invitrogen Life Technologies). Coculturing and Transwell assays were performed using 1×10^5 HIV-infected cell lines or 2×10^5 primary cells with 1×10^4 FDCs. For the FDC supernatant assay, filtered (0.2 μm) supernatants from FDC cultures were collected and added to HIV-1-infected cells at a 1:4 volume supernatant:total volume of fluid ratio. In the cell fixation assay, FDCs incubated with 3% paraformaldehyde in PBS for 2 h were washed three times with PBS and then twice with RPMI 1640 before coculturing.

Virus preparation and infection

$HIV\text{-}1_{JR\text{-}FL}$ or $HIV\text{-}1_{NL4\text{-}3}$ viruses were generated by transfection of the pJR-FL or pNL4-3 construct in 293T cells, respectively. Virus preparations were passed through a 0.4-μm filter and titrated using a conventional method as described previously (28). For the HIV-1 infection of primary cells, PBMCs were infected with $HIV\text{-}1_{JR\text{-}FL}$ for 24 h following stimulation with PHA-P (3 μg/ml) for 3 days. To adjust the culture condition for monocytes/macrophages with that for PBMCs, monocytes or macrophages were also infected with $HIV\text{-}1_{JR\text{-}FL}$ for 24 h following stimulation with PHA-P (3 μg/ml) for 3 days. All primary cell cultures were maintained in the absence of IL-2. Jurkat or FDCs were infected with $HIV\text{-}1_{NL\text{-}4\text{-}3}$ (multiplicity of infection (MOI) = 0.05) for 1, 3, or 5 days.

Antibodies

Polyclonal Abs raised against phospho-p65 (Ser^{536}), phospho-Syk (Tyr^{352}), phospho-IκBα (Ser^{32}), and unmodified Syk were purchased from Cell Signaling Technology. Anti-p65 polyclonal, actin, and PSGL-1 (KPL1) mAb were purchased from Santa Cruz Biotechnology. Anti-α-tubulin mAb was purchased from Sigma-Aldrich. Neutralizing Abs targeting PSGL-1 or ICAM-1 were purchased from R&D Systems. Anti-HIV-1 p24 mAb (2C2; mouse IgG1) was produced by Y. Tanaka (University of Ryukyus, Okinawa, Japan).

Isolation of total RNA from cells and quantitative RT-PCR

U1 cells and FDCs were harvested after coculturing and washed three times with PBS. Total RNA was then extracted using Isogen (Nippongene) according to the manufacturer's instructions. RNA (1 μg) was reverse transcribed using Superscript III (Invitrogen) before semiquantitative RT-PCR, and quantitative RT-PCR was performed using a SYBER Green One-step Real-time PCR kit (Invitrogen) with mRNA-specific primer pairs. Analyzed genes and corresponding primers are listed in supplemental Table I.[4]

Neutralization assay

HIV-1-infected cells were pretreated with neutralizing Abs (anti-PSGL-1, anti-ICAM-1, or control mouse IgG) for 2 h before and during coculturing. Optimal concentrations were determined by the IC_{50} values in accordance with the manufacturer's instructions. Culture supernatants were collected after 3 days and subjected to measurement of HIV-1 p24.

Chemicals and inhibitory assays

BAY11-7082 and JNK inhibitor II were purchased from Merck. The Syk-specific inhibitor ER-27319 (29, 30) was purchased from Sigma-Aldrich. Cells were pretreated with 30 μM ER-27319, 1 μM JNK inhibitor II, 1–2 μM BAY11-7082, or DMSO (Sigma-Aldrich) for 2 h. The inhibitor treated/untreated cells were then cocultured with FDCs in the presence of Syk or NF-κB inhibitor. In small interfering RNA (siRNA) experiments, U1 cells were transfected with control or PSGL-1 siRNA (Santa Cruz Biotechnology) by Nucleofector (Amaxa) and then cocultured with FDCs. Lysates and supernatants were collected from these cultures after 3 days for measurement of p24 and Western blotting analysis.

Flow cytometry

Cells were washed twice with staining buffer (3% FBS and 0.09% NaN_3/PBS) and then stained with PSGL-1-RP-E (BD Biosciences) for 30 min on ice. Cells were then washed twice and processed for flow cytometry.

Measurement of HIV-1 p24

Cell culture supernatants were collected after centrifugation at 4000 rpm for 5 min at 4°C and then processed for measurement of HIV-1 p24 by using Lumipulse (Fujirebio) according to the manufacturer's instructions. Assays were performed in triplicate.

Results

FDCs activate HIV-1 production in adjacent HIV-1-infected monocytic cells

To address whether FDCs can also activate HIV-1 replication in the surrounding infected monocytes/macrophages as an effective bystander or stimulator, several primary FDCs were established from fresh palatine tonsils of three healthy human donors (23).

[4] The online version of this article contains supplemental material.

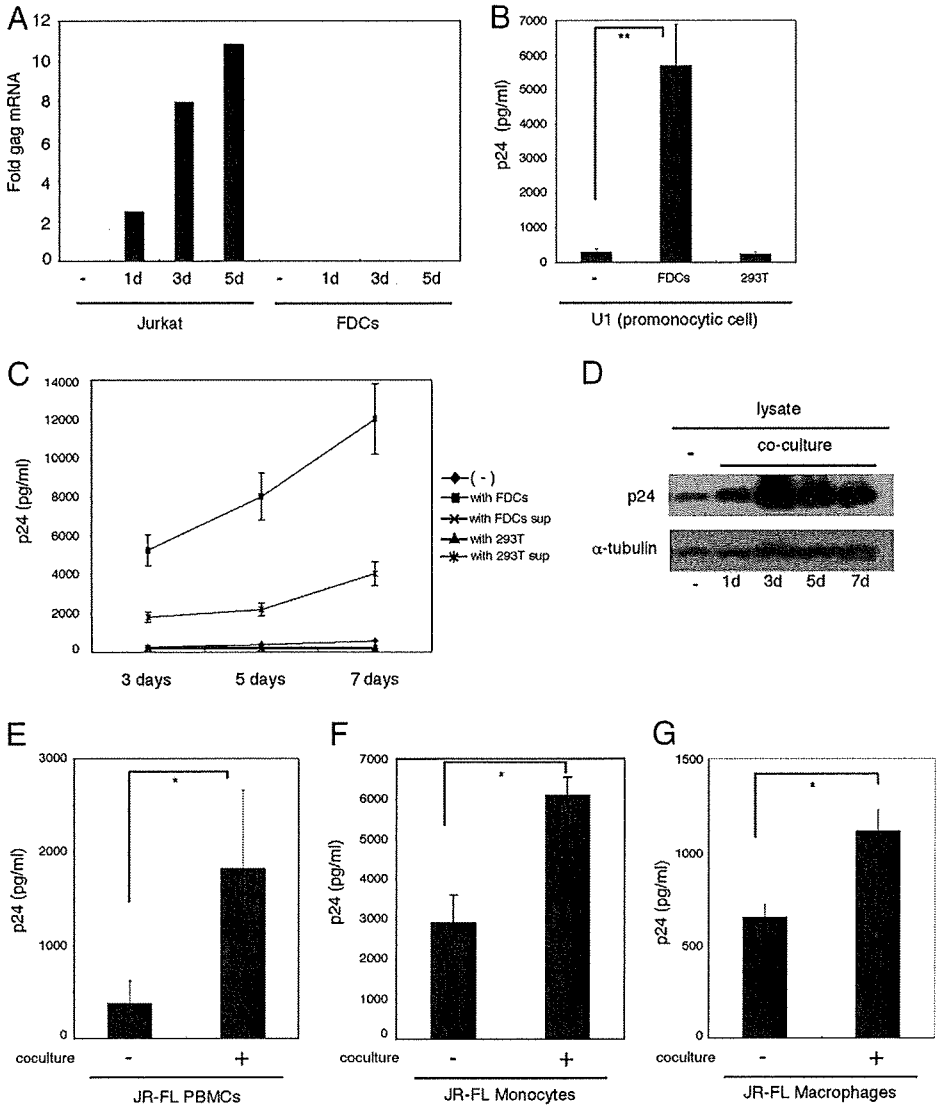

FIGURE 1. FDCs activate HIV-1 production in adjacent HIV-1-infected cells. *A*, Jurkat or FDCs were infected with HIV-1_{NL-4-3} (MOI = 0.05) for 1, 3, or 5 days. Cells were collected and then lysed for the separation of total RNA. Total RNA were treated with DNase I followed by quantitative RT-PCR with specific primer sets for either HIV-1 Gag or G3PDH. The data shown are the fold inductions normalized by G3PDH. *B*, U1 cells (1×10^5 cells/well) were cultured alone or in coculture with either FDCs or 293T cells (1×10^4 cells/well) for 3 days. Cell supernatants were then collected and assayed for measurement of p24. *C*, p24 levels in culture supernatants were monitored at 3, 5, and 7 days. *D*, p24 levels in lysates were monitored at 1, 3, 5, and 7 days by Western blot. *E*, PBMCs separated from a healthy donor were cultured with 3 μg/ml PHA for 3 days followed by infection with HIV-1_{JR-FL} (MOI = 0.05) for 24 h. The PBMCs (2×10^5 cells/well) were then cocultured with FDCs (1×10^4 cells/well) in the absence of IL-2 for 14 days. Culture supernatants were then assayed for measurement of p24. *F*, Monocytes separated from a healthy donor were cultured with 3 μg/ml PHA for 3 days followed by infection with HIV-1_{JR-FL} (MOI = 0.05) for 24 h. The monocytes (1×10^5 cells/well) were then cocultured with FDCs (1×10^4 cells/well) for 14 days. *G*, Primary differentiated macrophages were cultured with 3 μg/ml PHA for 3 days followed by infection with HIV-1_{JR-FL} (MOI = 0.05) for 24 h. The macrophages (1×10^5 cells/well) were then cocultured with FDCs (1×10^4 cells/well) for 7 days. Culture supernatants were then assayed for measurement of p24. The data shown in *B* are the average ± SD of at least three independent experiments. The data presented in *E–G* were obtained using samples of three donors (*, $p \leq 0.05$ and **, $p \leq 0.01$ by the Student *t* test).

Since each of these established cell lines was very similar in nature, exhibiting typical properties of FDCs (positive for CAN-42, S-100α, CD54, DC-SIGN, and CXCR4; morphological character such as spine-like spiculae and intercellular gap junction), the FDC 1 line was mainly used in subsequent experiments. FDCs themselves were not productively infected with HIV-1 (Fig. 1*A*), consistent with previous reports (22–25).

Initially, the FDCs were cocultured with chronically HIV-1-infected monocytic cell line U1 to examine whether they had the ability to activate HIV-1 replication. After 3 days of growth, HIV-1 production was analyzed for HIV-1 p24. The results showed that coculturing with FDCs significantly induced HIV-1 replication in the two infected cell types tested, whereas no such induction was observed when the U1 cells were cultured with 293T cells (Fig. 1*B*). A parallel kinetic study further demonstrated that the p24 levels in supernatants and lysates were increased in a time-dependent manner in U1 cells grown under these coculture conditions (Fig. 1, *C* and *D*). To address whether this trend occurred also in primary cells, FDCs were cocultured with PBMCs from healthy donors after infection with R5 (HIV-1_{JR-FL}) virus. As shown in Fig. 1*E*, the virus production was considerably augmented in coculture with FDCs. Furthermore, parallel experiments revealed that the virus production in monocytes or macrophages purified from PBMCs was also increased by coculturing with

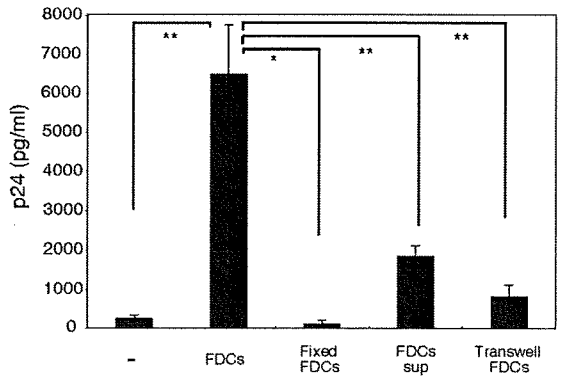

FIGURE 2. The enhancement of HIV-1 production by FDCs requires direct cell-cell interactions. U1 cells (1×10^5 cells/well) were cocultured with regular or paraformaldehyde-fixed FDCs (1×10^4 cells/well), cultured separately with FDCs on Transwell plates, or grown in medium supplemented with FDC culture supernatant at a 1:4 ratio of volume supernatant:total volume of fluid. Cell supernatants were collected after 3 days and assayed for measurement of p24. The data shown are the average ± SD of two independent experiments (*, $p \leq 0.05$ and **, $p \leq 0.01$ by the Student t test).

FDCs (Fig. 1, *F* and *G*). These data thus strongly indicate that FDCs can indeed activate viral replication monocytes/macrophages infected with HIV-1.

The enhancement of HIV-1 production by FDCs requires direct cell-cell interactions

To investigate whether this stimulation by FDCs was achieved by direct cell-cell interaction or soluble factors, we used two different cell culture methods for FDCs and U1 cells as follows: 1) FDCs were separately cultured with U1 cells using Transwells and 2) U1 cells were grown in culture medium supplemented with FDC supernatant. Although both culture systems could partially induce HIV-1 replication in U1 cells, these effects were ~20–30% of the full induction of those observed following coculture with FDCs (Fig. 2). This suggested that direct cell-cell interactions might be required for the full induction of HIV-1 replication in monocytic cells, although certain soluble factors may also activate HIV-1 replication to a lesser degree. Furthermore, the fixation of FDCs with paraformaldehyde before coculture completely abrogated the induction of HIV-1 replication in U1 cells, suggesting a requirement for bioactive cell surface molecules in this response.

Taken together, these data indicate that direct interactions via cell surface bioactive molecules are important to fully stimulate HIV-1 replication in monocytic U1 cells by FDCs.

Activation of NF-κB in both FDCs and HIV-1-infected cells following coculture

Our initial analysis demonstrated that FDCs can enhance HIV-1 replication in infected cells via cell-cell interaction. We thus examined whether this induction is initiated by the activation of the HIV-1 long-terminal repeat sequence (LTR). Quantitative and semiquantitative RT-PCR analyses revealed that the levels of HIV-1 mRNA were increased in U1 cells in tandem with increased supernatant p24 levels under coculture conditions with FDCs (Fig. 3, *A* and *B*).

HIV-1 replication has been shown to be regulated by host transcription factors such as NF-κB, NF-AT, Sp1, and AP-1 that are

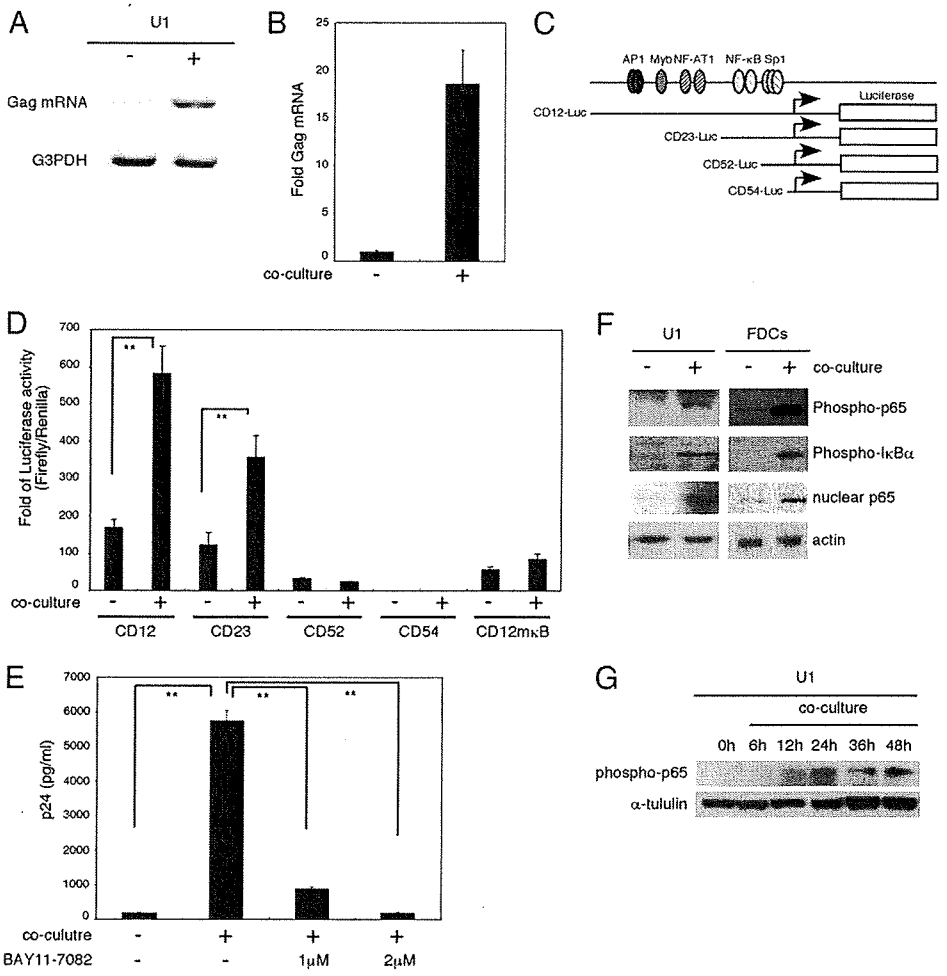

FIGURE 3. Activation of NF-κB in both FDCs and HIV-1-infected cells. *A* and *B*, U1 cells (1×10^5 cells/well) were cocultured with FDCs (1×10^4 cells/well) for 5 days and the mRNA levels for the indicated genes were measured by RT-PCR (*A*) or quantitative RT-PCR (*B*). *C*, Schematic representation of HIV-1 LTR-derived luciferase reporter constructs. *D*, U1 cells (1×10^5 cells/well) were initially transfected with the indicated reporter constructs and then cocultured with FDCs (1×10^4 cells/well) for 48 h, which was followed by a gene reporter assay. *E*, U1 cells (1×10^5 cells/well) were pretreated with the indicated concentrations of BAY 11-7082 for 2 h and then cocultured with FDCs (1×10^4 cells/well) for 3 days in the presence of the same concentration of BAY 11-7082. Cell supernatants were then collected and assayed for measurement of p24. *F*, U1 cells (1×10^5 cells/well) were cocultured with FDCs (1×10^4 cells/well) for 3 days and both cell types were collected and subjected to immunoblotting analysis for phospho-p65 (Ser^{536}), phospho-IκBα (Ser^{32}), p65, or actin. *G*, U1 cells (1×10^5 cells/well) were cocultured with FDCs (1×10^4 cells/well) and collected at the indicated time points. Cell lysates were subjected to immunoblot analysis using either phospho-p65 (Ser^{536}) or α-tubulin Abs. The data shown are the average ± SD of three independent experiments (*, $p \leq 0.05$ and **, $p \leq 0.01$ by the Student t test).

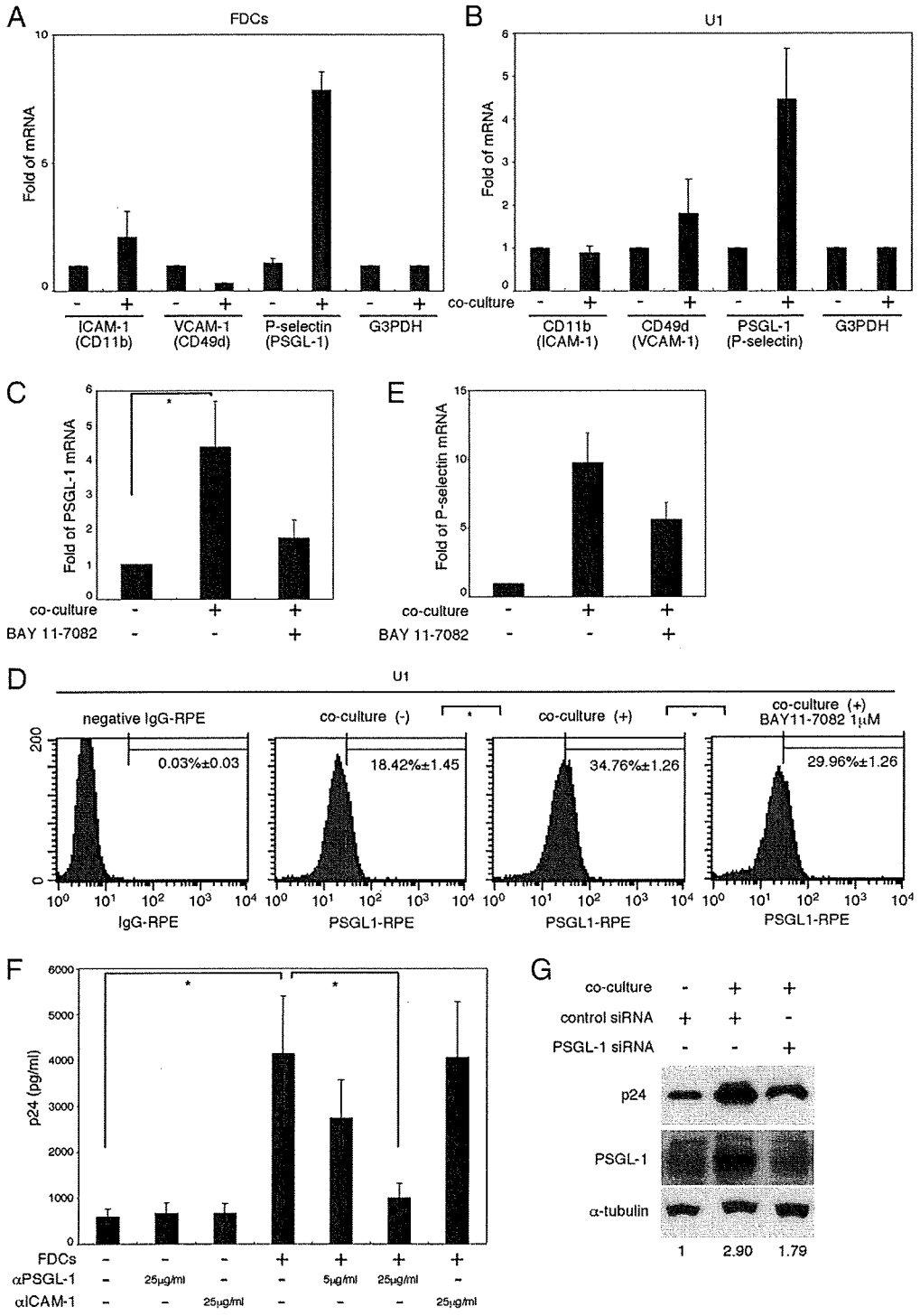

FIGURE 4. Involvement of P-selectin/PSGL-1 in reactivation of HIV-1 replication by FDC. *A* and *B*, U1 cells (1×10^5 cells/well) were cocultured with FDCs (1×10^4 cells/well) for 3 days. The mRNA levels of the indicated genes were then measured by quantitative RT-PCR. Labels inside parentheses indicate counterpart ligand or receptor molecules. *C–E*, U1 cells (1×10^5 cells/well) were cocultured with FDCs (1×10^4 cells/well) in the presence of BAY 11-7082 (1 μM) for 3 days and the levels of PSGL-1 in these cells were then analyzed by quantitative RT-PCR (*C*). Cell surface PSGL-1 was analyzed by flow cytometry using an anti-PSGL-1 Ab (*D*). M1 denotes the range of positive cell populations. *E*, P-selectin expression in FDCs analyzed by quantitative RT-PCR. *F*, U1 cells (1×10^5 cells/well) were untreated or pretreated with either PSGL-1 or ICAM-1 Ab for 1 h. Cells were then cocultured with FDCs (1×10^4 cells/well) for 3 days followed by measurement of p24. *G*, U1 cells (1×10^5 cells/well) were transduced with either control or PSGL-1 siRNA (final 6 nM) by Nucleofector according to the manufacturer's instructions. Cells were then cocultured with FDCs (1×10^4 cells/well) for 3 days followed by Western blot analysis with the indicated Abs. Numerical values below the blots indicate p24 signal intensities normalized by α-tubulin intensity derived by densitometry. The data shown are the average ± SD of three independent experiments (*, $p \leq 0.05$ and **, $p \leq 0.01$ by the Student *t* test).

recruited and bind directly to the HIV-1 LTR (31–33). To determine the identity of the *cis*-regulatory element(s) within the HIV-1 LTR that are the targets of FDC-mediated transcriptional activation, we examined various 5′-deletion mutants of these region as described in Fig. 3*C* (34). Coculturing of U1 cells with FDCs resulted in the activation of CD12 and CD23 reporter constructs

that harbor a NF-κB-binding sequence. However, the CD52 and CD54 constructs lacking this NF-κB consensus site were not activated, suggesting the involvement of NF-κB in the HIV-1 replication response (Fig. 3*D*). Consistent with this notion, the reporter construct CD12 that contains a site-directed mutation within the NF-κB binding site, CD12mκB, was not responsive to FDC stimulation. These results together indicate that the stimulation of HIV-1 in infected cells by FDCs is mediated via the activation of the HIV-1 LTR via NF-κB.

To further address this in terms of biological function, cells were treated with the NF-κB inhibitor BAY 11-7082 to further delineate the role of NF-κB in FDC-mediated HIV-1 replication. Treatment with BAY 11-7082 significantly suppressed HIV-1 production from U1 cells, even when growing in coculture with FDCs (Fig. 3*E*), although the viability of both cell types was not significantly affected by this exposure (data not shown). Taken together, our data thus indicate that intercellular communication pathways triggered by FDCs can promote and augment HIV-1 production in infected cells via NF-κB activation.

We next investigated whether NF-κB is in fact activated in FDCs as well as in U1 cells under coculture conditions. Consistent with our above gene reporter data, NF-κB activation was confirmed in U1 cells as revealed by the phosphorylation status of NF-κB p65 and IκBα (Fig. 3*F*). Interestingly, parallel experiments showed NF-κB activation in FDCs also in our coculture system, as revealed by immunoblotting with phospho-specific Abs (Fig. 3*F*). Furthermore, fractionation analysis demonstrated that the nuclear p65 (RelA) levels were significantly enhanced in both U1 and FDCs, indicating the nuclear accumulation of activated NF-κB (Fig. 3*F*). Parallel kinetic analysis revealed that NF-κB activation in U1 cells was initiated at 12 h and persisted for at least 48 h (Fig. 3*G*). These findings thus support our contention that cell-cell interactions between FDCs and U1 cells results in the constitutive activation of NF-κB in both cell types and that this is likely to be involved in the amplification of HIV-1 replication signals.

FDCs activate HIV-1 production via a P-selectin-PSGL-1 interaction

We were prompted to examine whether NF-κB up-regulates a specific cell surface ligand and its cognate receptor in FDCs and HIV-1-infected monocytic cells, eventually contributing to the amplification of HIV-1 replication signals via NF-κB activation. To this end, we examined the expression of different cell surface ligands and their cognate receptors which are known to be regulated by NF-κB. We chose three ligand/receptor combinations based upon a database search, ICAM-1/CD11b, VCAM-1/CD49d, and P-selectin/PSGL-1, and the expression of these molecules was analyzed by quantitative RT-PCR. Although the mRNA levels of ICAM-1 and VCAM-1 were not significantly altered upon stimulation, transcripts for P-selectin (CD62P/SLBP) were dramatically increased in FDCs (Fig. 4*A*). Interestingly, transcripts for the cognate receptor for P-selectin, PSGL-1, were found to be significantly up-regulated in U1 cells grown in coculture with the FDCs (Fig. 4*B*), but this was not the case for the CD11b and CD49d receptors. Quantitative RT-PCR and FACS analysis revealed that treatment with the NF-κB inhibitor BAY11-7082 significantly inhibited the increase of PSGL-1 mRNA expression and, consequently the cell surface expression of PSGL-1, in U1 cells cocultured with FDCs (Fig. 4, *C* and *D*). This suggested a crucial role for NF-κB signaling in the induction of PSGL-1 during this coculture in HIV-1-infected cells. Likewise, we found that BAY11-7082 treatment also decreased the induction of P-selectin mRNA in FDCs, indicating that the NF-κB activation in FDCs could play

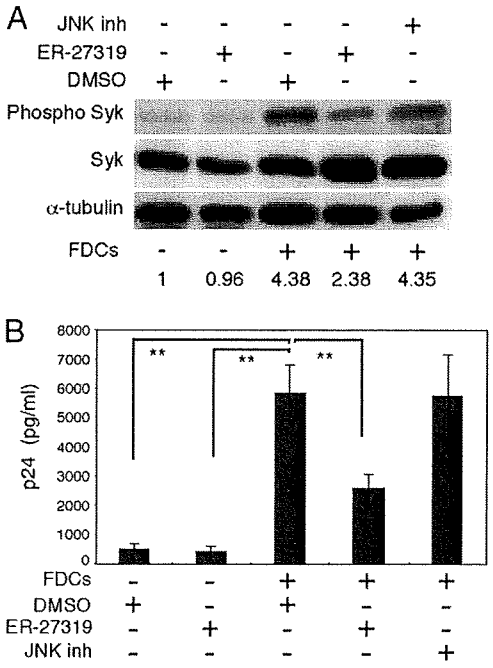

FIGURE 5. Syk is a mediator of P-selectin/PSGL-1 signaling for HIV-1 replication in U1 cells. *A* and *B*, U1 cells (1×10^5 cells/well) were untreated or pretreated with either ER-27319 (30 μM) or JNK inhibitor II (1 μM) for 1 h. Cells were then cocultured with FDCs (1×10^4 cells/well) for 3 days in the presence or absence of inhibitor. Cells were collected and subjected to immunoblotting analysis for phosphorylated Syk (Tyr^{352}), unmodified Syk, and α-tubulin (*A*). The numbers below the blot indicate the band intensity ratios. Cell supernatants were assayed for measurement of p24 (*B*). The data shown are the average ± SD of two independent experiments (*, $p \leq 0.05$ and **, $p \leq 0.01$ by the Student *t* test).

a crucial role in the induction of P-selectin during the coculture with HIV-1-infected monocytic cells (Fig. 4*E*).

Next, to test the biological significance of a P-selectin-PSGL-1 interaction in terms of HIV-1 induction in our FDC coculture system, U1 cells were pretreated with blocking Ab against PSGL-1 before setting up these cultures. Treatment with PSGL-1 Ab, but not an ICAM-1 Ab, specifically suppressed HIV-1 production in a dose-dependent manner (Fig. 4*F*). Consistent with this result, targeted disruption of PSGL-1 by specific siRNA significantly decreased HIV-1 production in U1 cells coculturing with FDCs (Fig. 4*G*). These results together indicate that a juxtacrine signaling mechanism mediated by PSGL-1/P-selectin underlies the activation of HIV-1 replication in infected monocytic cells stimulated by FDCs.

Syk acts as a downstream effector of PSGL-1 during HIV-1 replication

Several previous reports have demonstrated that the cytoplasmic domain of PSGL-1 can directly interact with a Src family kinase, the Syk (35). Syk consists of two N-terminal Src homology 2 domains, which bind phosphorylated ITAM sequences, and a C-terminal tyrosine kinase domain (35–37). The phosphorylation of Syk at Tyr^{352} has been shown to be a hallmark of its activation. Indeed, phosphorylated Syk was found in our present analyses to be significantly increased in U1 cells during their cocultivation with FDCs (Fig. 5*A*).

To next examine the possible biological functions of Syk during HIV-1 replication, we used a specific inhibitor of the molecule ER-27319 (29, 30) in our FDC cocultures. Treatment with ER-27319 significantly decreased HIV-1 production and this was accompanied by a reduction in the phosphorylated Syk levels in U1

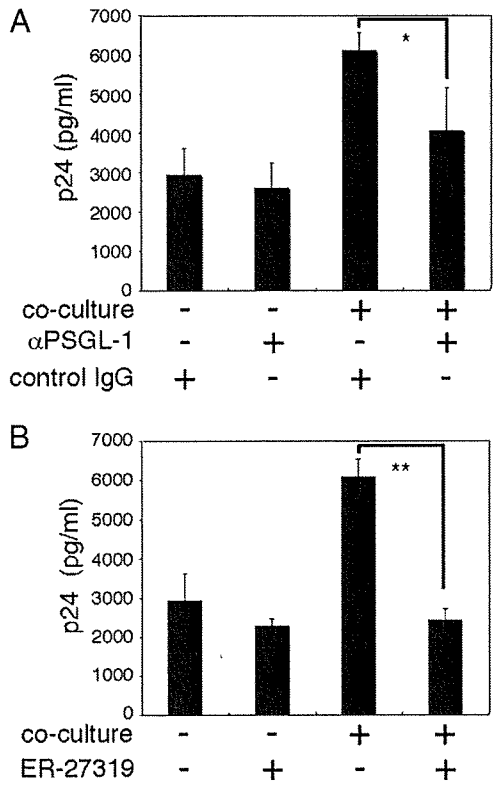

FIGURE 6. Inhibition of the PSGL-1/Syk pathway abrogates FDC-induced HIV-1 replication in primary monocytes. *A* and *B*, Primary human monocytes were separated from three healthy donors as indicated in *Materials and Methods* and these cells were then treated with 3 μg/ml PHA for 3 days. After stimulation, the cells (1×10^5 cells/well) were infected with HIV-$1_{JR\text{-}FL}$ (MOI = 0.05) for 24 h and subsequently cocultured with FDCs (1×10^4 cells/well) in the presence of PSGL-1 Ab (25 μg/ml; *A*) or ER-27319 (30 μM; *B*) at 14 days, followed by measurement of p24 (*, $p \leq 0.05$ and **, $p \leq 0.01$ by the Student *t* test).

cells (Fig. 5), whereas JNK inhibitor II had no such effects. These results indicate that the juxtacrine signaling between FDCs and HIV-1-infected monocytic cells mediated by P-selectin/PSGL-1 results in the activation of Syk, which serves as a mediator of the function of NF-κB activation in the HIV-1 replication pathway.

PSGL-1 and Syk inhibition blocks FDC-induced HIV-1 replication in primary monocytes

Finally, we addressed whether FDCs can also activate HIV-1 production in infected primary cells via P-selectin/PSGL-1 pathway, in this case human primary monocytes from healthy donors that had subsequently been exposed to HIV-$1_{JR\text{-}FL}$. At 24 h after viral infection, the primary monocytes were cocultured with FDCs in the presence or absence of either PSGL-1 Ab or the Syk inhibitor ER-27319. Both of these treatments significantly inhibited HIV-1 production in the primary monocytes in a manner similar to U1 cells (Fig. 6). These results indicate that similar to U1 cells, the PSGL-1/Syk signaling is likely to be a major pathway mediating FDC-induced HIV-1 replication in primary monocytes.

Discussion

Previous studies have indicated that HIV-1 infection is largely confined to the GCs of secondary lymph nodes where FDCs commonly reside (15–17). This microenvironment could thus provide the site for highly productive HIV-1 infection whereby FDCs might execute "on-switch" signaling to increase HIV replication. Furthermore, cell-cell infection appears to be far more efficient for viral spread than cell-free virus infection (38, 39). We here report that FDCs can facilitate HIV-1 replication in adjacent infected monocytes/macrophages via a cell-cell interaction mechanism.

FDCs have been shown to interact with B or $CD4^+$ T cells in the GCs of normal lymph nodes (16, 17, 20). It is also reported that in tonsils, $CD150\ (SLAM)^+$ monocytes were localized not only in T cell areas, but also within GCs, suggesting they play a role in B cell activation (40). Moreover, substantial numbers of HIV-infected macrophages were observed in GCs during the course of HIV infection (41). Thus, FDCs can interact with HIV-infected monocytes or macrophages under these conditions during HIV-1 infection. Furthermore, the dysfunctional FDC network is observed in secondary lymph nodes of lymphadenopathy, where the degeneration of the FDC network is usually seen following highly active antiretroviral therapy or administration of therapeutic vaccine in HIV or SIV infection (42–45). One of the most common histological features of HIV-1-associated lymphadenopathy is hyperplastic lymphoid follicles that subsequently undergoes follicululysis, in which FDCs can be scattered to the extra-GC within the lymph nodes such as cortical sinuses and mantle bodies (46, 47). Our results with immunohistochemical analysis indicate that FDCs reside with various types of HIV-1-infected cells including monocytes or macrophages in lymphoid organs of HIV-1-associated lymphadenopathy (supplemental Fig. 1). Therefore, our current proposed model for cell-cell interaction between FDCs and HIV-1-infected monocytic cells may reflect the biological or pathological aspects of the natural HIV infection in vivo. However, we could not determine the specific cell surface molecules for activating HIV-1 replication via the cell-cell interaction in vivo. Moreover, it is not well confirmed whether a multitude of other cells, cytokines, and other factors in vivo could influence the cell-cell interaction observed in our in vitro coculture system. Further careful analysis should be performed using human tissues as well as a humanized mouse model inoculated with HIV-1-infected human cells.

We clearly demonstrated here that FDCs, derived from human tonsils, can enhance HIV-1 production in infected monocytic cells in a coculture system. This enhancement requires direct cell-cell interactions via a juxtacrine signaling pathway that is mediated by P-selectin/PSGL-1. Our results are summarized as follows: 1) FDCs can activate HIV-1 replication in infected cells through cell-cell interactions; 2) HIV-1 replication is activated at the transcriptional level and is accompanied by the activation of the HIV-1 LTR through NF-κB; 3) P-selectin expression in FDCs and the up-regulation of its cognate receptor PSGL-1 in HIV-1-infected monocytes cells are facilitated via NF-κB activation; 4) the pathways leading to HIV-1 induction in cell lines also function in human primary monocytes and macrophages infected with HIV-1; and 5) selective inhibitors of PSGL-1 or Syk can efficiently block HIV-1 production in U1 and primary monocytes. These data together indicate for the first time that FDCs are a potent inducer of HIV-1 replication in surrounding infected monocytes and macrophages and that PSGL-1/Syk signaling plays a crucial role in this induction of HIV-1.

Very recently, Thacker et al. (26) reported a similar but distinct role of FDCs in the induction of HIV-1 replication in $CD4^+$ T cells obtained from PBMCs and GCs. We also confirmed that FDCs could stimulate HIV-1 replication in MOLT-4 T cells (23) as well as in primary $CD4^+$ T cells (data not shown). However, FDCs-induced HIV-1 replication in $CD4^+$ T cells might be mediated by a distinct mechanism from HIV-1-infected monocytic cells since the involvement of the PSGL-1/Syk pathway in $CD4^+$ T cells was found to be not prominent (K. Ohba, A. Ryo, and N. Yamamoto, unpublished observation). Therefore, the molecular mechanism for

FDCs to stimulate HIV-1 replication in surrounding infected cells could be attributable to cell type specific.

Intercellular interactions via a ligand/receptor juxtacrine signaling system has been implicated in several virus infections. Tsukamoto et al. (48) reported that the juxtacrine function of the IL-15/IL-15 receptor system in human B cell lines might play a role in the infectivity of EBV (48). Pilotti et al. (49) have demonstrated a crucial protective role for CCL3L1/CCL3 (MIP-1αP/LD78α) signals in both HIV infection and subsequent disease progression. These intercellular communication processes may play an important role in the sustained infection of viruses in different microenvironments within lymphoid organs. Further careful analyses will be required in the future to elucidate the variety of intercellular communication systems that may operate during HIV-1 infection.

There is now some evidence for a role of PSGL-1 as a signal-transmitting receptor in neutrophils (50), monocytes (51), and T lymphocytes (52). This molecule has been reported to associate with Syk through its interaction with moesin and promotes the tyrosine phosphorylation and thus the activation of Syk (35). In addition, signals elicited through PSGL-1/Syk can induce the activation of downstream effectors such as ERK, c-Fos, and NF-κB (53). The activation of NF-κB via PSGL-1 has also been demonstrated in platelet-stimulated monocytes, although the details of the molecular pathways leading to NF-κB activation in this manner have not yet been elucidated (51). Consistent with this result also, we found from our current analyses that PSGL-1/Syk signaling can activate NF-κB. This observation suggests a linkage between PSGL-1 signaling and HIV-1 replication through the activation of NF-κB.

Recently, Gilbert et al. (54) have reported that Src and Syk tyrosine kinases play important roles in the spread of HIV-1 from immature monocyte-derived DCs to $CD4^+$ T cells. They found that these kinases play a suppressive role in virus transfer in vitro probably by inhibiting the formation of the virological synapse. However, it has not been well characterized whether these signaling molecules contribute to the cell-cell interaction between HIV-1-infected cells and adjacent noninfected cells for virus replication. We showed in this current study that the activation of Syk through the PSGL-1 positively regulates HIV-1 replication in infected monocytic cells. Thus, Syk could be involved at multiple points in HIV-1 infection and its role could be dependent on each step of HIV-1 life cycle.

In summary, we demonstrate in our current study that FDCs are a potent activator of HIV-1 replication in surrounding infected monocytic cells. Furthermore, the PSGL-1/Syk pathway is important for this activation of HIV-1 replication. These results shed valuable new light on our understanding of the natural progression of HIV-1 infection over the long term and could provide a means for designing novel therapeutic interventions against AIDS and related disorders.

Acknowledgments

We thank S. Yamaoka and W. Sugiura for helpful discussions and H. Shimura, N. Sakamaki, C. Matsubara, M. Tanaka, and H. Soeda for technical assistance.

Disclosures

The authors have no financial conflict of interest.

References

1. Stevenson, M. 2003. HIV-1 pathogenesis. *Nat. Med.* 9: 853–860.
2. Pope, M., and A. T. Haase. 2003. Transmission, acute HIV-1 infection and the quest for strategies to prevent infection. *Nat. Med.* 9: 847–852.
3. Matsuyama, T., Y. Hamamoto, T. Okamoto, K. Shimotohno, N. Kobayashi, and N. Yamamoto. 1988. Tumour necrosis factor and HIV: a note of caution. *Lancet* 2: 1364.
4. Matsuyama, T., N. Kobayashi, and N. Yamamoto. 1991. Cytokines and HIV infection: is AIDS a tumor necrosis factor disease? *AIDS* 5: 1405–1417.
5. Kinter, A., J. Arthos, C. Cicala, and A. S. Fauci. 2000. Chemokines, cytokines and HIV: a complex network of interactions that influence HIV pathogenesis. *Immunol. Rev.* 177: 88–98.
6. Kedzierska, K., S. M. Crowe, S. Turville, and A. L. Cunningham. 2003. The influence of cytokines, chemokines and their receptors on HIV-1 replication in monocytes and macrophages. *Rev. Med. Virol.* 13: 39–56.
7. Pantaleo, G., C. Graziosi, J. F. Demarest, L. Butini, M. Montroni, C. H. Fox, J. M. Orenstein, D. P. Kotler, and A. S. Fauci. 1993. HIV infection is active and progressive in lymphoid tissue during the clinically latent stage of disease. *Nature* 362: 355–358.
8. Pierson, T., J. McArthur, and R. F. Siliciano. 2000. Reservoirs for HIV-1: mechanisms for viral persistence in the presence of antiviral immune responses and antiretroviral therapy. *Annu. Rev. Immunol.* 18: 665–708.
9. Han, Y., M. Wind-Rotolo, H. C. Yang, J. D. Siliciano, and R. F. Siliciano. 2007. Experimental approaches to the study of HIV-1 latency. *Nat. Rev. Microbiol.* 5: 95–106.
10. Pauza, C. D. 1988. HIV persistence in monocytes leads to pathogenesis and AIDS. *Cell. Immunol.* 112: 414–424.
11. Igarashi, T., C. R. Brown, Y. Endo, A. Buckler-White, R. Plishka, N. Bischofberger, V. Hirsch, and M. A. Martin. 2001. Macrophage are the principal reservoir and sustain high virus loads in rhesus macaques after the depletion of $CD4^+$ T cells by a highly pathogenic simian immunodeficiency virus/HIV type 1 chimera (SHIV): Implications for HIV-1 infections of humans. *Proc. Natl. Acad. Sci. USA* 98: 658–663.
12. Moser, B., and P. Loetscher. 2001. Lymphocyte traffic control by chemokines. *Nat. Immunol.* 2: 123–128.
13. Cahalan, M. D., and G. A. Gutman. 2006. The sense of place in the immune system. *Nat. Immunol.* 7: 329–332.
14. Bieniasz, P. D. 2004. Intrinsic immunity: a front-line defense against viral attack. *Nat. Immunol.* 5: 1109–1115.
15. Allen, C. D., T. Okada, and J. G. Cyster. 2007. Germinal-center organization and cellular dynamics. *Immunity* 27: 190–202.
16. Szakal, A. K., Y. Aydar, P. Balogh, and J. G. Tew. 2002. Molecular interactions of FDCs with B cells in aging. *Semin. Immunol.* 14: 267–274.
17. van Nierop, K., and C. de Groot. 2002. Human follicular dendritic cells: function, origin and development. *Semin. Immunol.* 14: 251–257.
18. Victoratos, P., J. Lagnel, S. Tzima, M. B. Alimzhanov, K. Rajewsky, M. Pasparakis, and G. Kollias. 2006. FDC-specific functions of p55TNFR and IKK2 in the development of FDC networks and of antibody responses. *Immunity* 24: 65–77.
19. Tew, J. G., J. Wu, M. Fakher, A. K. Szakal, and D. Qin. 2001. Follicular dendritic cells: beyond the necessity of T-cell help. *Trends Immunol.* 22: 361–367.
20. Li, L., and Y. S. Choi. 2002. Follicular dendritic cell-signaling molecules required for proliferation and differentiation of GC-B cells. *Semin. Immunol.* 14: 259–266.
21. Lee, I. Y., E. M. Ko, S. H. Kim, D. I. Jeoung, and J. Choe. 2005. Human follicular dendritic cells express prostacyclin synthase: a novel mechanism to control T cell numbers in the germinal center. *J. Immunol.* 175: 1658–1664.
22. Keele, B. F., L. Tazi, S. Gartner, Y. Liu, T. B. Burgon, J. D. Estes, T. C. Thacker, K. A. Crandall, J. C. McArthur, and G. F. Burton. 2008. Characterization of the follicular dendritic cell reservoir of human immunodeficiency virus type 1. *J. Virol.* 82: 5548–5561.
23. Taruishi, M., K. Terashima, Z. Dewan, N. Yamamoto, S. Ikeda, D. Kobayashi, Y. Eishi, M. Yamazaki, T. Furusaka, M. Sugimoto, et al. 2004. Role of follicular dendritic cells in the early HIV-1 infection: in vitro model without specific antibody. *Microbiol. Immunol.* 48: 693–702.
24. Burton, G. F., B. F. Keele, J. D. Estes, T. C. Thacker, and S. Gartner. 2002. Follicular dendritic cell contributions to HIV pathogenesis. *Semin. Immunol.* 14: 275–284.
25. Grouard, G., and E. A. Clark. 1997. Role of dendritic and follicular dendritic cells in HIV infection and pathogenesis. *Curr. Opin. Immunol.* 9: 563–567.
26. Thacker, T. C., X. Zhou, J. D. Estes, Y. Jiang, B. F. Keele, T. S. Elton, and G. F. Burton. 2009. Follicular dendritic cells and human immunodeficiency virus type 1 transcription in $CD4^+$ T cells. *J. Virol.* 83: 150–158.
27. Folks, T. M., J. Justement, A. Kinter, C. A. Dinarello, and A. S. Fauci. 1987. Cytokine-induced expression of HIV-1 in a chronically infected promonocyte cell line. *Science* 238: 800–802.
28. Watanabe, S., K. Terashima, S. Ohta, S. Horibata, M. Yajima, Y. Shiozawa, M. Z. Dewan, Z. Yu, M. Ito, T. Morio, et al. 2007. Hematopoietic stem cell-engrafted NOD/SCID/IL2Rγ null mice develop human lymphoid systems and induce long-lasting HIV-1 infection with specific humoral immune responses. *Blood* 109: 212–218.
29. Moriya, K., J. Rivera, S. Odom, Y. Sakuma, K. Muramato, T. Yoshiuchi, M. Miyamoto, and K. Yamada. 1997. ER-27319, an acridone-related compound, inhibits release of antigen-induced allergic mediators from mast cells by selective inhibition of Fcε receptor I-mediated activation of Syk. *Proc. Natl. Acad. Sci. USA* 94: 12539–12544.
30. Andrews, R. P., C. L. Kepley, L. Youssef, B. S. Wilson, and J. M. Oliver. 2001. Regulation of the very late antigen-4-mediated adhesive activity of normal and nonreleaser basophils: roles for Src, Syk, and phosphatidylinositol 3-kinase. *J. Leukocyte Biol.* 70: 776–782.
31. Cullen, B. R. 1991. Regulation of HIV-1 gene expression. *FASEB J.* 5: 2361–2368.

32. Rohr, O., C. Marban, D. Aunis, and E. Schaeffer. 2003. Regulation of HIV-1 gene transcription: from lymphocytes to microglial cells. *J. Leukocyte Biol.* 74: 736–749.
33. Okamoto, T., T. Matsuyama, S. Mori, Y. Hamamoto, N. Kobayashi, N. Yamamoto, S. F. Josephs, F. Wong-Staal, and K. Shimotohno. 1989. Augmentation of human immunodeficiency virus type 1 gene expression by tumor necrosis factor α. *AIDS Res. Hum Retroviruses* 5: 131–138.
34. Takada, N., T. Sanda, H. Okamoto, J. P. Yang, K. Asamitsu, L. Sarol, G. Kimura, H. Uranishi, T. Tetsuka, and T. Okamoto. 2002. RelA-associated inhibitor blocks transcription of human immunodeficiency virus type 1 by inhibiting NF-κB and Sp1 actions. *J. Virol.* 76: 8019–8030.
35. Urzainqui, A., J. M. Serrador, F. Viedma, M. Yanez-Mo, A. Rodriguez, A. L. Corbi, J. L. Alonso-Lebrero, A. Luque, M. Deckert, J. Vazquez, and F. Sanchez-Madrid. 2002. ITAM-based interaction of ERM proteins with Syk mediates signaling by the leukocyte adhesion receptor PSGL-1. *Immunity* 17: 401–412.
36. Fodor, S., Z. Jakus, and A. Mocsai. 2006. ITAM-based signaling beyond the adaptive immune response. *Immunol. Lett.* 104: 29–37.
37. Underhill, D. M., and H. S. Goodridge. 2007. The many faces of ITAMs. *Trends Immunol.* 28: 66–73.
38. Dimitrov, D. S., R. L. Willey, H. Sato, L. J. Chang, R. Blumenthal, and M. A. Martin. 1993. Quantitation of human immunodeficiency virus type 1 infection kinetics. *J. Virol.* 67: 2182–2190.
39. Chancey, C. J., K. V. Khanna, J. F. Seegers, G. W. Zhang, J. Hildreth, A. Langan, and R. B. Markham. 2006. Lactobacilli-expressed single-chain variable fragment (scFv) specific for intercellular adhesion molecule 1 (ICAM-1) blocks cell-associated HIV-1 transmission across a cervical epithelial monolayer. *J. Immunol.* 176: 5627–5636.
40. Farina, C., D. Theil, B. Semlinger, R. Hohlfeld, and E. Meinl. 2004. Distinct responses of monocytes to Toll-like receptor ligands and inflammatory cytokines. *Int. Immunol.* 16: 799–809.
41. Eitner, F., Y. Cui, G. Grouard-Vogel, K. L. Hudkins, A. Schmidt, T. Birkebak, M. B. Agy, S. L. Hu, W. R. Morton, D. M. Anderson, et al. 2000. Rapid shift from virally infected cells to germinal center-retained virus after HIV-2 infection of macaques. *Am. J. Pathol.* 156: 1197–1207.
42. Gray, C. M., J. Lawrence, E. A. Ranheim, M. Vierra, M. Zupancic, M. Winters, J. Altman, J. Montoya, A. Zolopa, J. Schapiro, et al. 2000. Highly active antiretroviral therapy results in HIV type 1 suppression in lymph nodes, increased pools of naive T cells, decreased pools of activated T cells, and diminished frequencies of peripheral activated HIV type 1-specific $CD8^+$ T cells. *AIDS Res. Hum Retroviruses* 16: 1357–1369.
43. Lu, W., X. Wu, Y. Lu, W. Guo, and J. M. Andrieu. 2003. Therapeutic dendritic-cell vaccine for simian AIDS. *Nat. Med.* 9: 27–32.
44. Schmitz, J., J. van Lunzen, K. Tenner-Racz, G. Grossschupff, P. Racz, H. Schmitz, M. Dietrich, and F. T. Hufert. 1994. Follicular dendritic cells retain HIV-1 particles on their plasma membrane, but are not productively infected in asymptomatic patients with follicular hyperplasia. *J. Immunol.* 153: 1352–1359.
45. Zhang, Z. Q., T. Schuler, W. Cavert, D. W. Notermans, K. Gebhard, K. Henry, D. V. Havlir, H. F. Gunthard, J. K. Wong, S. Little, et al. 1999. Reversibility of the pathological changes in the follicular dendritic cell network with treatment of HIV-1 infection. *Proc. Natl. Acad. Sci. USA* 96: 5169–5172.
46. Baroni, C. D., and S. Uccini. 1990. Lymph nodes in HIV-positive drug abusers with persistent generalized lymphadenopathy: histology, immunohistochemistry, and pathogenetic correlations. *Prog. AIDS Pathol.* 2: 33–50.
47. Houn, H. Y., A. A. Pappas, and E. M. Walker, Jr. 1990. Lymph node pathology of acquired immunodeficiency syndrome (AIDS). *Ann. Clin. Lab. Sci.* 20: 337–342.
48. Tsukamoto, K., Y. C. Huang, W. C. Dorsey, B. Carns, and V. Sharma. 2006. Juxtacrine function of interleukin-15/interleukin-15 receptor system in tumour derived human B-cell lines. *Clin. Exp. Immunol.* 146: 559–566.
49. Pilotti, E., L. Elviri, E. Vicenzi, U. Bertazzoni, M. C. Re, S. Allibardi, G. Poli, and C. Casoli. 2007. Postgenomic up-regulation of CCL3L1 expression in HTLV-2-infected persons curtails HIV-1 replication. *Blood* 109: 1850–1856.
50. Hidari, K. I., A. S. Weyrich, G. A. Zimmerman, and R. P. McEver. 1997. Engagement of P-selectin glycoprotein ligand-1 enhances tyrosine phosphorylation and activates mitogen-activated protein kinases in human neutrophils. *J. Biol. Chem.* 272: 28750–28756.
51. Weyrich, A. S., T. M. McIntyre, R. P. McEver, S. M. Prescott, and G. A. Zimmerman. 1995. Monocyte tethering by P-selectin regulates monocyte chemotactic protein-1 and tumor necrosis factor-α secretion: signal integration and NF-κB translocation. *J. Clin. Invest.* 95: 2297–2303.
52. Damle, N. K., K. Klussman, M. T. Dietsch, N. Mohagheghpour, and A. Aruffo. 1992. GMP-140 (P-selectin/CD62) binds to chronically stimulated but not resting $CD4^+$ T lymphocytes and regulates their production of proinflammatory cytokines. *Eur. J. Immunol.* 22: 1789–1793.
53. Tada, J., M. Omine, T. Suda, and N. Yamaguchi. 1999. A common signaling pathway via Syk and Lyn tyrosine kinases generated from capping of the sialomucins CD34 and CD43 in immature hematopoietic cells. *Blood* 93: 3723–3735.
54. Gilbert, C., C. Barat, R. Cantin, and M. J. Tremblay. 2007. Involvement of Src and Syk tyrosine kinases in HIV-1 transfer from dendritic cells to $CD4^+$ T lymphocytes. *J. Immunol.* 178: 2862–2871.

Biochemical and Biophysical Research Communications 381 (2009) 294–299

Contents lists available at ScienceDirect

Biochemical and Biophysical Research Communications

journal homepage: www.elsevier.com/locate/ybbrc

The prolyl isomerase Pin1 stabilizes the human T-cell leukemia virus type 1 (HTLV-1) Tax oncoprotein and promotes malignant transformation

Soo-Jin Jeong, Akihide Ryo *, Naoki Yamamoto *

AIDS Research Center, National Institute of Infectious Diseases, 1-23-1 Toyama, Shinjuku-ku, Tokyo 162-8640, Japan

ARTICLE INFO

Article history:
Received 6 February 2009
Available online 11 February 2009

Keywords:
Pin1
Tax
Protein stability
Ubiquitination
Transformation

ABSTRACT

The HTLV Tax protein is crucial for viral replication and malignant transformation. We investigated the possible role of peptidyl prolyl isomerase Pin1 in the positive regulation of the human T-cell leukemia virus type 1 Tax. Pin1 is highly expressed in adult T-cell leukemia (ATL) cells expressing Tax protein and forced expression of Pin1 in turn increases the Tax protein expression. Pin1 prolonged the protein half-life of Tax by suppressing the ubiquitination and subsequent lysosomal degradation of Tax. Pin1 interacts with phosphorylated Tax on its Ser160-Pro motif at the mitotic phase. Finally, we found that Pin1 plays a supporting role in Tax-mediated cell transformation. Our current study demonstrates an important role for Pin1 in the post-translational regulation of Tax and suggests that the targeting of Pin1 may offer a new insight into the pathogenesis of HTLV-1 related diseases.

Introduction

The peptidyl-prolyl *cis/trans* isomerase (PPIase) Pin1 binds only to phospho-Ser/Thr-Pro motifs on its substrate proteins, thereby catalyzing the *cis/trans* isomerization of the peptide bond and acting as a post-phosphorylation catalyst in the regulation of protein function [1]. Pin1 is highly expressed in various cancers and its deregulation of Pin1 may play a pivotal role in these diseases [1,2]. For instance, it has been reported that Pin1 positively regulates both colorectal and mammary tumorigenesis by increasing β-catenin and cyclin D1 expression [3]. Also, our recent studies have demonstrated that Pin1 acts as a putative anti-apoptotic molecule by the negative regulating Daxx in malignant tumor cells [4].

Human T-cell leukemia virus type 1 (HTLV-1) is the etiologic agent of the aggressive and fatal malignancy of CD4+ lymphocytes known as adult T-cell leukemia (ATL) [5]. During the carrier state in HTLV-1-mediated malignancies such as ATL, the oncoprotein Tax has been shown to play an essential role in the cell proliferation and oncogenesis [6]. Tax is a 40-kDa viral regulatory protein and plays critical roles in the activation of various cellular genes and for viral gene expression, replication and transformation [7]. Tax is a phosphoprotein with a predominately nuclear subcellular localization that accomplishes multiple functions via protein–protein interactions [8].

In our current study, we have investigated the regulation of Tax by Pin1 through phosphorylation-dependent prolyl isomerization. Our results demonstrate that Pin1 physically interacts with Tax, especially during the mitotic phase there by inhibiting both the ubiquitination and the lysosomal degradation of Tax. We also demonstrate that the phosphorylation of Tax on Ser160-Pro motif by mitotic kinase(s) is crucial for both its interaction with Pin1 and its prolonged stabilization. Of importance, a soft agar colony transformation assay using CTLL-2 cells demonstrated that Pin1 increases the transformation activity of Tax whereas the targeted inhibition of Pin1 significantly suppressed the Tax-mediated cell transformation. Hence, our current data provide the evidence that Pin1 plays a critical role in the post-translational regulation of HTLV-1 Tax.

Materials and methods

Cells. HTLV-1-transformed cells and T-lymphocytes were maintained in RPMI supplemented with 10% fetal calf serum, 2 μM L-glutamine and penicillin/streptomycin. 293T cells were maintained in DMEM supplemented with 10% fetal calf serum, 2 μM L-glutamine and penicillin/streptomycin. Mouse T-lymphocyte CTLL-2 cells were kindly provided by Dr. Masahiro Fujii (Niigata University, Japan) and maintained in RPMI supplemented with 10% fetal calf serum, 1 nM IL-2, 50 nM 2-ME, 2 μM L-glutamine and penicillin/streptomycin.

Transfection and luciferase assay. Transient transfections were carried out using Effectene Transfection Reagent (Qiagen). Luciferase assays have been described previously [9].

RT-PCR. Total RNA was isolated using the RNeasy Mini kit (Qiagen). RT-PCR was performed using the Takara one-step RT-PCR kit, following the manufacturers' instructions.

* Corresponding authors. Fax: +81 3 5285 1165 (N. Yamamoto).
E-mail addresses: aryo@nih.go.jp (A. Ryo), nyama@nih.go.jp (N. Yamamoto).

0006-291X/$ - see front matter © 2009 Elsevier Inc. All rights reserved.
doi:10.1016/j.bbrc.2009.02.024

Protein degradation assay. Protein degradation assays were performed as described previously [10]. Briefly, cycloheximide (100 μg/ml) was added to the medium 24 h after cell transfection, and the cells were harvested at different time points.

In vitro and in vivo protein binding assays. GST pull-down and co-immunoprecipitation assay were carried out as described previously [4].

Cell cycle analyses. Cell cycle was analyzed for DNA content using FACSCalibur (Becton Dickinson Bioscience). Cells were stained with propidium idodide (50 μg/ml) after RNase treatment as described previously [11].

Colony formation assay. Colony formation assays were performed with CTLL-2 cells infected with retrovirus carrying pMRX-ires-blst-Tax and/or pMRX-ires-puro-Pin1, and pMRX-ires-blst-Tax and/or pSuper-retro-puro-Pin1 siRNA in soft agar media using a CytoSelect 96-well cell transformation assay kit (Cell Biolabs) according to the manufacturer's instructions.

Results

Pin1 increases HTLV-1 Tax-mediated transactivation

To examine whether Pin1 influences Tax-mediated transcriptional activation, 293T cells were transiently transfected with luciferase reporter constructs, HTLV-1 LTR- or NF-κB-Luc in the absence or presence of Tax and/or Pin1. As expected, the expression of Tax increased the activation of both the HTLV-1 LTR and NF-κB (Fig. 1A and B, lane 2). In contrast, the expression of Pin1 had no significant effect upon the viral LTR and NF-κB (lane 3). Interestingly, the co-expression of Tax and Pin1 produced a significant increase in the reporter activity for both HTLV-1 LTR- and NF-κB-Luc, indicating that Pin1 increases Tax-mediated transcriptional activation (lane 4). These data were further confirmed in HTLV-1-transformed Hut 102 cells expressing endogenous Tax (Fig. 1C). Hut 102 cells infected with a retroviral vector carrying Pin1 siRNA decreased the HTLV-1 LTR luciferase activity compared with cells infected with control siRNA. These data thus demonstrate that Pin1 enhances Tax-mediated transactivation in HTLV-1-transformed cells.

Pin1 overexpression facilitates the protein stability of HTLV-1 Tax

Next, we sought to examine the expression of Pin1 in HTLV-1-transformed cells and T-lymphocytes (Fig. S1A). Pin1 was found to be highly expressed in Tax-expressing HTLV-1-transformed cells M8166, Hut 102, MT-1, MT-2 and MT-4 compared with Tax-non-expressing HTLV-1-transformed cells ATL-43Tb(−) and T-lymphocytes Jurkat, Molt-4 and CEM cells. To further confirm this contention, we performed Western blot analysis and RT-PCR using 293T/Pin1 siRNA cells transfected with Pin1 and Tax. Pin1 significantly increased the protein expression of Tax in a dose-dependent manner (Fig. S1B) but the Tax mRNA levels showed no significant change (Fig. S1C). These results suggest that Pin1 regulates the expression of the Tax protein via a post-translational mechanism.

To analyze whether Pin1 can stabilize the Tax protein, we performed a protein degradation assay by treating cells with cycloheximide (CHX). First, 293T cells stably expressing either control or Pin1 siRNA cells were transiently co-transfected with Tax and HA-LacZ as an internal control (Fig. 2A). Cycloheximide was then added 24 h post-transfection. Cells were collected at 0, 2, 4, 6 or 8 h and Western blot analyses were performed for Tax, Pin1 and HA-LacZ. This experiment revealed that the protein stability of Tax was significantly reduced in 293T/Pin1 siRNA cells compared with control cells, indicating that Pin1 indeed enhances the protein stability of Tax. Consistent with this result, the stability of Tax was found to be restored by Pin1 overexpression in 293T/Pin1 siRNA cells (Fig. 2B).

Two different pathways, proteasome- and lysosome-dependent, are principally responsible for intracellular protein degradation [12]. To address whether Tax degradation is mediated by either pathway, we performed parallel experiments using either the proteasome inhibitor MG-132 or the lysosome inhibitor NH_4Cl (Fig. S2A). Treatment with NH_4Cl significantly inhibited the rapid degradation of Tax in 293T/Pin1 siRNA cells, whereas the treat-

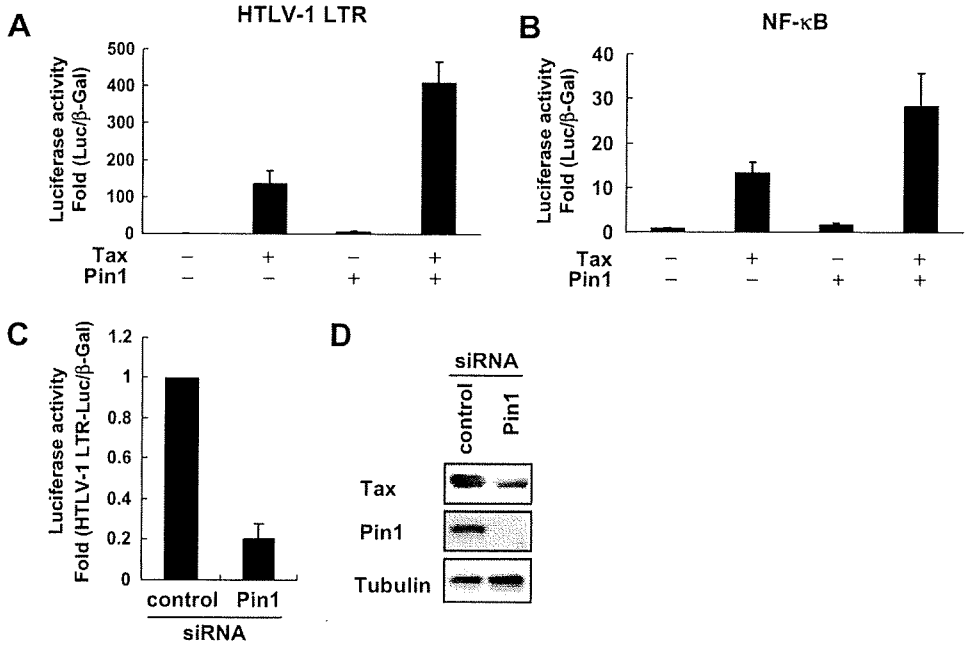

Fig. 1. Pin1 enhances HTLV-1 Tax-mediated transcriptional activation. (A,B) 293T cells were transiently transfected with plasmids expressing Tax, Pin1 and the reporter constructs HTLV-1 LTR- (A) or NF-κB-Luc (B). (C) Hut 102 cells were infected with either control or Pin1 siRNA molecules using the pSuper-Retro-puro-vector and then transiently transfected with HTLV-1 LTR-Luc. Forty-eight hours post-transfection, cells were collected and luciferase activities were measured. Luciferase values were adjusted for transfection efficiency using RSV β-galactosidase. (D) Western blot analysis of Hut 102 cells was performed for Tax, Pin1 and tubulin.

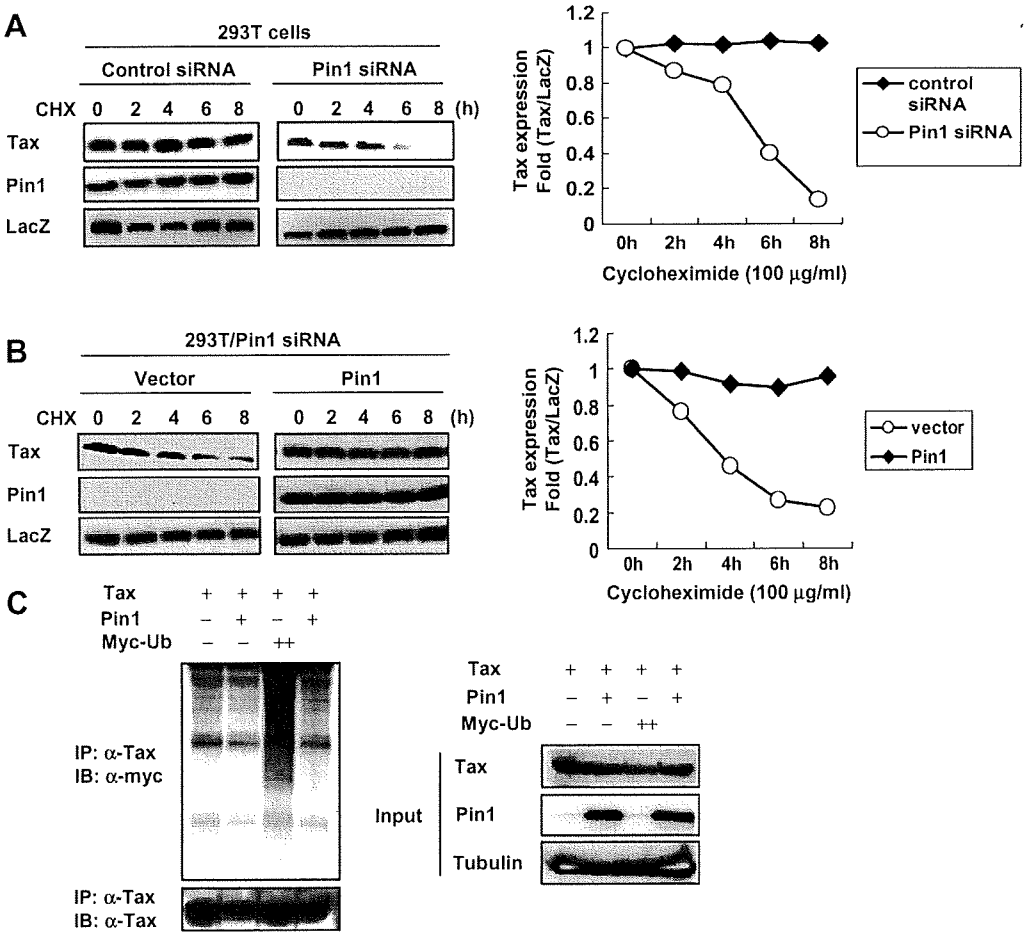

Fig. 2. Pin1 overexpression inhibits both the degradation and the ubiquitination of Tax. (A,B) 293T cells stably expressing control siRNA or Pin1 siRNA molecules were transfected with Tax and HA-LacZ (A). 293T/Pin1 siRNA cells were transfected with empty vector or Pin, Tax and HA-LacZ (B). Cells were treated with cycloheximide (CHX) after 24 h, and harvested at the indicated time points. This was followed by Western blotting analysis with anti-Tax, Pin1 and HA antibodies. The data from the quantitative analyses are shown in the graphs. (C) 239T cells were transfected with either empty vector or Tax in the absence or presence of Myc-Ub. Whole cell lysates were immunoprecipitated with anti-Tax or anti-Myc and immunoblotted with these same antibodies.

ment with MG-132 did not prolong the protein half-life of Tax compared with DMSO control. Additional lysosome inhibitors (leupeptin and chloroquine) further confirmed that the protein degradation of Tax is lysosome-dependent (Fig. S2B).

Pin1 overexpression inhibits the ubiquitination of Tax

To explore the effects of Pin1 upon the ubiquitination of Tax immunoprecipitation analyses of 293T/Pin1 siRNA cells transfected with Tax and/or Pin1 in the absence or presence of ubiquitin revealed that Pin1 overexpression blocks the ubiquitination of Tax (Fig. 2C). In an additional experiment to examine the importance of Pin1 in the suppression of Tax ubiquitination, HTLV-1-transformed Hut 102 cells were treated with the Pin1 inhibitor Juglone or infected with retroviral Pin1 siRNA and processed for immunoblot analysis with anti-Tax antibody which allow the detection of both wild type and ubiquitinated Tax (Fig. S3). The results indicated an increase in the level of polyubiquitinated Tax resulting from the blockage of Pin1. Our data thus confirm that Pin1 suppresses the destabilization and also the ubiquitination of Tax.

Pin1 interacts with Tax during the mitotic phase

The interaction between Tax and Pin1 was determined by GST pull-down assay. The results demonstrate that GST-Pin1, but not GST interacts with Tax in cell lysates derived from DMSO control cells (Fig. 3A). Of interest, this interaction was significantly increased when cells had been treated with nocodazole (M-phase blocker), but not with hydroxyurea (G1–S-phase blocker), suggesting that cell cycle arrest at mitotic phase facilitates this interaction.

The results of a co-immunoprecipitation assay provide further evidence for the interaction between Pin1 and Tax (Fig. 3B). Hut 102 cells were incubated with or without nocodazole to induce mitotic arrest and immunoprecipitated with either control IgG or anti-Pin1 antibody. The results demonstrate that a significant interaction between Pin1 and Tax occurs at the mitotic phase. The mitotic arrest of cell cycle with nocodazole was determined by the level of cyclin B1 (Fig. 3B) and flow cytometry analysis (Fig. 3C), respectively. In addition, the interaction between Pin1 and Tax was significantly decreased by the treatment with alkaline phosphatase (AP), suggesting that Pin1 binds to only phosphorylated Tax (Fig. S4A). A parallel analysis of Tax and Pin1 binding was performed to test whether either the binding or catalytic activity of Pin1 is necessary for the interaction between Pin1 and Tax. We used 293T/Pin1 siRNA cells transfected with Tax and either empty vector, Pin1 wild type or the Pin1 mutants W34A (WWdomain mutant) and K63A (PPIase domain mutant) (Fig. S4B). The results demonstrate that the WW domain of Pin1 is required for the binding to Tax.

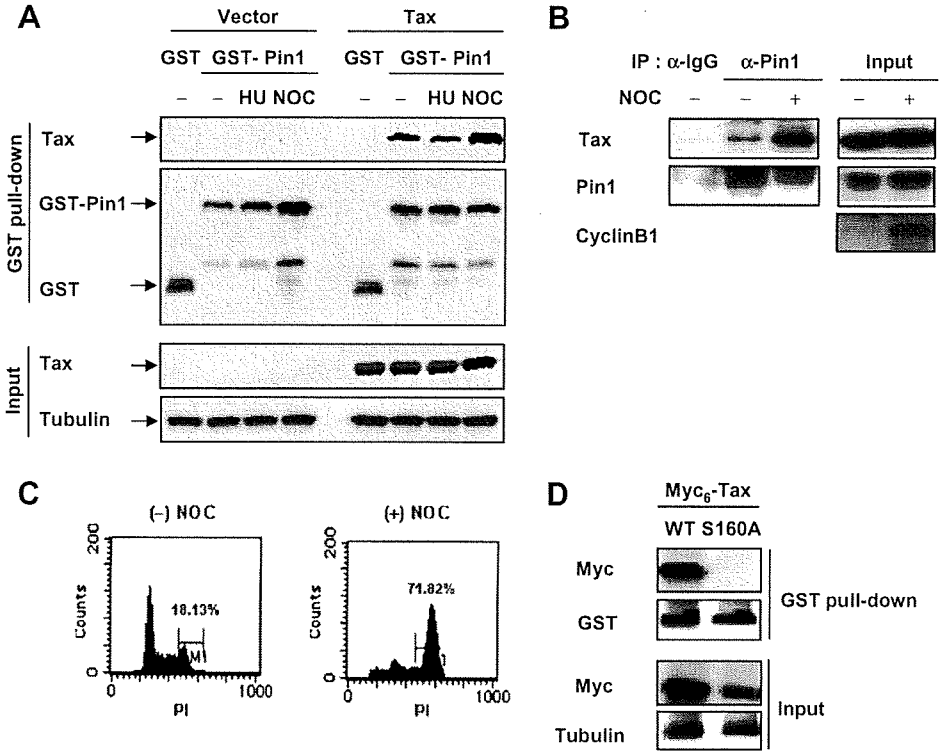

Fig. 3. Pin1 physically interacts with phosphorylated Tax in the mitotic phase *in vitro* and *in vivo*. (A) 293T cells were transfected with either empty vector or Tax and treated with hydroxyurea (HU) or nocodazole (NOC). Cell lysates were prepared, subjected to a pull-downed with purified GST or GST-Pin1 and immunoblotted with anti-Tax and GST antibodies. (B) Hut 102 cells were treated with or without NOC. Whole cell lysates were immunoprecipitated with IgG control or anti-Pin1 antibody and then immunoblotted with anti-Tax and anti-Pin1 antibodies. (C) Hut 102 cells treated with or without NOC were fixed in 70% ethanol, stained with propidium iodide (PI) and their cell cycle distribution was analyzed by flow cytometry. (D) 293T cells were transfected with Myc_6-Tax wild type or the Tax S160A mutant for 48 h. Cell lysates were prepared, pulled-down with purified GST or GST-Pin1 and immunoblotted with anti-Myc and GST antibodies. A Western blot for Tax and tubulin is also shown.

The HTLV-1 Tax Ser160-Pro motif is important for the interaction with Pin1 and subsequent protein stabilization by Pin1

To identify the region of Tax that binds to Pin1, we generated several Tax deletion mutants (Fig. S5A). Results of the GST pull-down assay shown in Fig. S5B indicate that Pin1 binds to Tax in the region between amino acids 157 and 190. Pin1 binds to only phosphorylated Ser/Thr-Pro motifs within its target proteins [1,13]. Since there is only single site of Ser/Thr-Pro motif (Ser160-Pro161) between amino acids 157 and 190 in Tax, we introduced a site-specific mutation into Ser160 site by substitution of Ala for Ser (S160A). GST pull-down analysis revealed that Pin1 does not bind to Tax S160A, indicating that Pin1 binds to phosphorylated Ser160-Pro motif of Tax (Fig. 3D). In addition, cycloheximide analysis demonstrated that Pin1 fails to stabilize the S160A mutant of Tax (Fig. S6A). Mutant S160A decreased the transcription of both HTLV-1 LTR and NF-κB by 50% compared with wild type Tax, suggesting that the phosphorylation of Tax on Ser-160-Pro motif indeed plays a role in regulating the transactivation of HTLV-1 LTR (Figs. S6B and C).

Taken together, these data suggest that the direct interaction between Pin1 and Tax via the Ser 160-Pro motif suppresses the degradation of Tax and thereby enhances its transcriptional activity.

Pin1 promotes Tax-mediated transformation in CTLL-2 cells

Cellular transformation assay was performed using the mouse T-lymphocytes CTLL-2 cells, which are interleukin (IL)-2 dependent cells to explore whether Pin1 can regulate Tax-mediated transformation. Results showed that CTLL-2 cells infected with retroviral Tax alone showed increased their transformation whereas Pin1 alone had no detectable effect (Fig. 4A). Significantly, co-infection with the retroviral Tax and Pin1 vectors resulted in an increase in transformation, suggesting that Pin1 positively affects the Tax-mediated transformation of CTLL-2 cells. We found by Western blot analysis that Tax expression was stabilized in the presence of Pin1.

A parallel assay was performed to further confirm the importance of Pin1 for Tax-mediated transformation using CTLL-2 cells infected with retroviral vectors expressing either control or Pin1 siRNA and Tax. The results showed that the suppression of Pin1 significantly decreased the transformation efficiency of Tax (Fig. 4B). Taken together, these results indicate that Pin1 plays a positive role in the induction of Tax-mediated transformation via its stable interaction with HTLV-1 Tax protein.

Discussion

The peptidyl prolyl isomerase Pin1 regulates a variety of cellular processes, including cell growth, cell cycle progression and cellular stress responses [14,15] and is linked to the progression of several diseases, including cancer, Alzheimer's disease and asthma [1,13,16,17]. In this regard, it is of interest that in recent studies Pin1 has also been shown to play an important role in virus-related diseases [18,19]. Of interest, Pelopenese et al. reported that Pin1 interacts with the HTLV-1 Tax which is a key factor in leukemogenesis and modulates its activation of NF-κB [20]. In agreement with this study, we also show that Pin1 binds to phosphorylated Tax and positively regulates the stabilization of Tax, thus promoting Tax-mediated transformation. In addition, we identified a novel phosphorylation site on Ser160 of Tax and showed that it is targeted

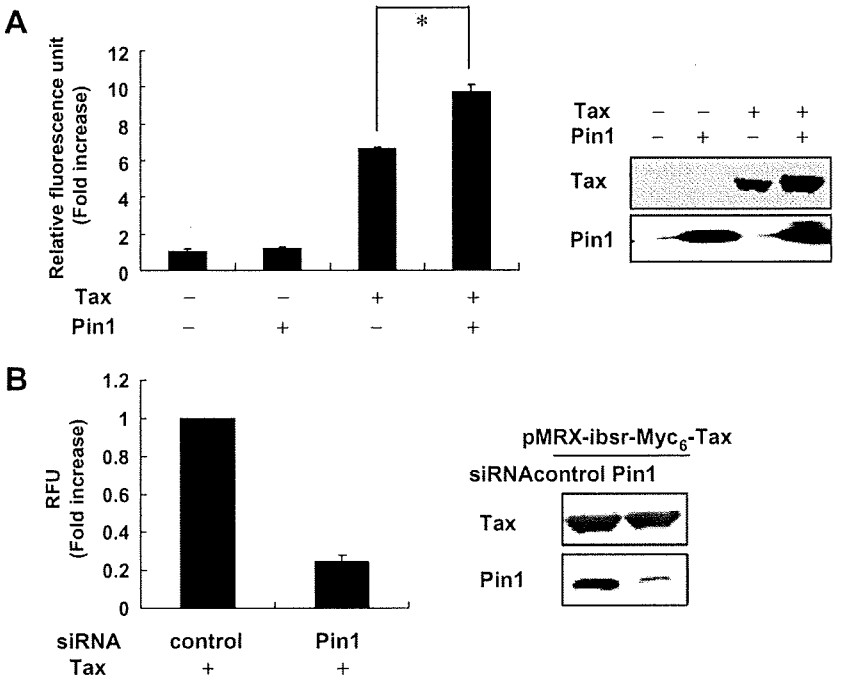

Fig. 4. Pin1 promotes the transformation of CTLL-2 cells by Tax. CTLL-2 mouse T-lymphocytes were infected with retroviruses expressing Tax and/or Pin1 (A) and control or Pin1 siRNA, and Tax (B) and incubated in soft agar media for 6–8 days. The formation of colonies was detected with the plate reader using a 485/520 nm filter set. A Western blot analysis for Pin1 and Tax is also shown. Asterisk means the value of Student's *t*-test ($^{*}p < 0.001$).

by Pin1-mediated prolyl isomerization by a mapping of Tax binding region to Pin1.

It was recently reported that, by phosphoryl mapping of Tax that both positive and negative phosphorylation signals for this protein result in the maintenance of an "active" subfraction, suggesting the importance of phosphorylation in the regulation of Tax activity [21]. However, it has not been well characterized how the activity of Tax is further regulated by phosphorylation in the cells. Our data demonstrate that Pin1 fails to stabilize a Tax mutant with alanine substitution at Ser160 (S160A), suggesting that the interaction between Pin1 and Tax is critical for the protein stability of Tax. Similarly, it has been demonstrated previously that Pin1 directly binds to phosphorylated cyclin D1 that has been phosphorylated by glycogen synthase kinase-3β (GSK-3β) and thereby prevents its nuclear export and ubiquitin-mediated degradation of cyclin D1 [22]. Pin1 also targets the phosphorylated Thr254-Pro motif of NF-κB p65 and inhibits the binding of p65 and IκB, which subsequently prevents its degradation by a ubiquitin-mediated pathway [10].

Intracellular protein stabilization is mainly regulated by the ubiquitin-proteasome pathway [23]. Several studies have been shown that Tax is ubiquitinated and physically interacts with the proteasome [24–26]. Of interest, Chiari et al. reported that Tax is not degraded by ubiquitination and that Tax conjugation to ubiquitin in fact mediates a non-proteolytic function of this protein [24]. Our current data suggest that the degradation of Tax is accomplished by a ubiquitin-dependent lysosomal pathway. The degradation of Tax was blocked by the treatment with the lysosome inhibitors NH_4Cl, leupeptin and chloroquine, but not by the proteasome inhibitors MG-132, MG-115 and lactacystin. Importantly, we observed that Pin1 overexpression inhibits the ubiquitination of Tax, further indicating that Pin1 prevents Tax degradation via the ubiquitin–lysosome pathway. Marques et al. previously reported the ubiquitin-dependent lysosomal degradation of the 3-hydroxy-nonenal (HNE)-modified protein in lens epithelial cells [27]. The authors in this study speculated that the ubiquitin-conjugating system may serve as a common mechanism for recognizing various types of modified or damaged proteins. These ubiquitinated proteins can then be degraded by either the proteasome or through lysosomes although the mechanisms underlying the different fates of these ubiquitinated proteins remain unclear.

Because the HTLV-1 Tax protein is essential for the cellular transformation as well as viral replication [7], it was important from a clinical perspective to identify the mechanisms underlying the activities of this protein. To elucidate the physiological role of Pin1 in the regulation of Tax, we performed a colony transformation assay using CTLL-2 primary mouse T-lymphocytes. Our results demonstrate that Pin1 promotes Tax-mediated cellular transformation and also stabilizes the Tax protein.

In conclusion, we herein demonstrated a novel regulatory mechanism for HTLV-1 Tax that is mediated via Pin1-catalyzed-phosphorylation-dependent prolyl isomerization. Phosphorylation of Tax at Ser160-Pro motif promotes its interaction with Pin1 during the mitotic phase of cell cycle, which stabilizes the Tax protein by inhibiting its ubiquitination and thereby promotes malignant transformation. Further studies will be required to identify the specific kinase(s) responsible for phosphorylation of the Ser160-Pro Pin1 binding motif of Tax. Our present analyses suggest that the targeting of Pin1 may offer a new insight into the pathogenesis and treatment of HTLV-1 related diseases.

Acknowledgments

This study was supported in part by grants from the Japanese Ministries of Education, Culture, Sports, Science and Technology (20390136, 13226027, 14406009 and 1941075) Health, Labour and Welfare (H18-005) and Human Health Science (H19-001) to N.Y. and A.R.

Appendix A. Supplementary data

Supplementary data associated with this article can be found, in the online version, at doi:10.1016/j.bbrc.2009.02.024.

References

[1] K.P. Lu, Y.C. Liou, X.Z. Zhou, Pinning down proline-directed phosphorylation signaling, Trends Cell Biol. 12 (2002) 164–172.
[2] L. Bao, A. Kimzey, G. Sauter, J.M. Sowadski, K.P. Lu, D.G. Wang, Prevalent overexpression of prolyl isomerase Pin1 in human cancers, Am. J. Pathol. 164 (2004) 1727–1737.
[3] J. Kuramochi, T. Arai, S. Ikeda, J. Kumagai, H. Uetake, K. Sugihara, High Pin1 expression is associated with tumor progression in colorectal cancer, J. Surg. Oncol. 94 (2006) 155–160.
[4] A. Ryo, A. Hirai, M. Nishi, Y.C. Liou, K. Perrem, S.C. Lin, H. Hirano, S.W. Lee, I. Aoki, A suppressive role of the prolyl isomerase Pin1 in cellular apoptosis mediated by the death-associated protein Daxx, J. Biol. Chem. 282 (2007) 36671–36681.
[5] B.J. Poiesz, F.W. Ruscetti, A.F. Gazdar, P.A. Bunn, J.D. Minna, R.C. Gallo, Detection and isolation of type C retrovirus particles from fresh and cultured lymphocytes of a patient with cutaneous T-cell lymphoma, Proc. Natl. Acad. Sci. USA 77 (1980) 7415–7419.
[6] M. Matsuoka, Human T-cell leukemia virus type I and adult T-cell leukemia, Oncogene 22 (2003) 5131–5140.
[7] T. Akagi, H. Ono, K. Shimotohno, Characterization of T cells immortalized by Tax1 of human T-cell leukemia virus type 1, Blood 86 (1995) 4243–4249.
[8] O.J. Semmes, K.T. Jeang, Mutational analysis of human T-cell leukemia virus type I Tax: regions necessary for function determined with 47 mutant proteins, J. Virol. 66 (1992) 7183–7192.
[9] S.J. Jeong, M. Radonovich, J.N. Brady, C.A. Pise-Masison, HTLV-I Tax induces a novel interaction between p65/RelA and p53 that results in inhibition of p53 transcriptional activity, Blood 104 (2004) 1490–1497.
[10] A. Ryo, F. Suizu, Y. Yoshida, K. Perrem, Y.C. Liou, G. Wulf, R. Rottapel, S. Yamaoka, K.P. Lu, Regulation of NF-kappaB signaling by Pin1-dependent prolyl isomerization and ubiquitin-mediated proteolysis of p65/RelA, Mol. Cell 12 (2003) 1413–1426.
[11] S.J. Jeong, A. Dasgupta, K.J. Jung, J.H. Um, A. Burke, H.U. Park, J.N. Brady, PI3K/AKT inhibition induces caspase-dependent apoptosis in HTLV-1-transformed cells, Virology 370 (2008) 264–272.
[12] T. Hideshima, J.E. Bradner, D. Chauhan, K.C. Anderson, Intracellular protein degradation and its therapeutic implications, Clin. Cancer Res. 11 (2005) 8530–8533.
[13] A. Ryo, Y.-C. Liou, K.P. Lu, G. Wulf, Prolyl isomerase Pin1: a catalyst for oncogenesis and a potential therapeutic target in cancer, J. Cell Sci. 116 (2003) 773–783.
[14] P. Rudrabhatla, Y.L. Zheng, N.D. Amin, S. Kesavapany, W. Albers, H.C. Pant, Pin1 dependent prolyl isomerization modulates the stress induced phosphorylation of high molecular weight neurofilament protein (NF-H), J. Biol. Chem. (2008) 26737–26747.
[15] P. Zacchi, M. Gostissa, T. Uchida, C. Salvagno, F. Avolio, S. Volinia, Z. Ronai, G. Blandino, C. Schneider, G. Del Sal, The prolyl isomerase Pin1 reveals a mechanism to control p53 functions after genotoxic insults, Nature 419 (2002) 853–857.
[16] P.J. Lu, G. Wulf, X.Z. Zhou, P. Davies, K.P. Lu, The prolyl isomerase Pin1 restores the function of Alzheimer-associated phosphorylated tau protein, Nature 399 (1999) 784–788.
[17] Z.J. Shen, S. Esnault, L.A. Rosenthal, R.J. Szakaly, R.L. Sorkness, P.R. Westmark, M. Sandor, J.S. Malter, Pin1 regulates TGF-beta1 production by activated human and murine eosinophils and contributes to allergic lung fibrosis, J. Clin. Invest. 118 (2008) 479–490.
[18] R. Pang, T.K. Lee, R.T. Poon, S.T. Fan, K.B. Wong, Y.L. Kwong, E. Tse, Pin1 interacts with a specific serine-proline motif of hepatitis B virus X-protein to enhance hepatocarcinogenesis, Gastroenterology 132 (2007) 1088–1103.
[19] K. Watashi, M. Khan, V.R. Yedavalli, M.L. Yeung, K. Strebel, K.T. Jeang, Human immunodeficiency virus-1 replication and regulation of APOBEC3G by peptidyl prolyl isomerase Pin1, J. Virol. (2008) 9928–9936.
[20] J.-M. Peloponese Jr., J. Yasunaga, T. Kinjo, K. Watashi, K.-T. Jeang, Peptidylproline cis–trans isomerase Pin1 interacts with HTLV-1 Tax and modulates its activation of NF-{kappa}B, J. Virol. (2009) (JVI.01824-08).
[21] S.S. Durkin, M.D. Ward, K.A. Fryrear, O.J. Semmes, Site-specific phosphorylation differentiates active from inactive forms of the human T-cell leukemia virus type 1 Tax oncoprotein, J. Biol. Chem. 281 (2006) 31705–31712.
[22] Y.C. Liou, A. Ryo, H.K. Huang, P.J. Lu, R. Bronson, F. Fujimori, T. Uchida, T. Hunter, K.P. Lu, Loss of Pin1 function in the mouse causes phenotypes resembling cyclin D1-null phenotypes, Proc. Natl. Acad. Sci. USA 99 (2002) 1335–1340.
[23] A. Hershko, A. Ciechanover, The ubiquitin system, Annu. Rev. Biochem. 67 (1998) 425–479.
[24] E. Chiari, I. Lamsoul, J. Lodewick, C. Chopin, F. Bex, C. Pique, Stable ubiquitination of human T-cell leukemia virus type 1 tax is required for proteasome binding, J. Virol. 78 (2004) 11823–11832.
[25] J.M. Peloponese Jr., H. Iha, V.R. Yedavalli, A. Miyazato, Y. Li, K. Haller, M. Benkirane, K.T. Jeang, Ubiquitination of human T-cell leukemia virus type 1 tax modulates its activity, J. Virol. 78 (2004) 11686–11695.
[26] R. Rousset, C. Desbois, F. Bantignies, P. Jalinot, Efects on NF-kappa B1/p105 processing of the interaction between the HTLV-1 transactivator Tax and the proteasome, Nature 381 (1996) 328–331.
[27] C. Marques, P. Pereira, A. Taylor, J.N. Liang, V.N. Reddy, L.I. Szweda, F. Shang, Ubiquitin-dependent lysosomal degradation of the HNE-modified proteins in lens epithelial cells, FASEB J. 18 (2004) 1424–1426.

FEBS Letters 583 (2009) 1243–1250

ELSEVIER

FEBS Letters

journal homepage: www.FEBSLetters.org

Requirement for microtubule integrity in the SOCS1-mediated intracellular dynamics of HIV-1 Gag

Mayuko Nishi [a,b], Akihide Ryo [a,b,*], Naomi Tsurutani [c], Kenji Ohba [a], Tatsuya Sawasaki [d], Ryo Morishita [d], Kilian Perrem [e], Ichiro Aoki [b], Yuko Morikawa [c], Naoki Yamamoto [a,*]

[a] AIDS Research Center, National Institute of Infectious Diseases, 1-23-1 Toyama, Shinjuku-ku, Tokyo, Japan 162-8640, Japan
[b] Department of Pathology, Yokohama City University School of Medicine, 3-9 Fuku-ura, Kanazawa-ku, Yokohama 236-0004, Japan
[c] Kitasato Institute for Life Sciences, Kitasato University, Shirokane 5-9-1, Minato-ku, Tokyo 108-8641, Japan
[d] Cell Free Science and Research Center, Ehime University, Ehime 790-8577, Japan
[e] CSIRO, P.O. Box 225, Dickson ACT 2602, Australia

ARTICLE INFO

Article history:
Received 8 December 2008
Revised 16 March 2009
Accepted 18 March 2009
Available online 25 March 2009

Edited by Kaspar Locher

Keywords:
HIV
Host factor
Suppressor of cytokine signaling 1
Microtubule
Ubiquitin
Trafficking

ABSTRACT

Suppressor of cytokine signaling 1 (SOCS1) is a recently identified host factor that positively regulates the intracellular trafficking and stability of HIV-1 Gag. We here examine the molecular mechanism by which SOCS1 regulates intercellular Gag trafficking and virus particle production. We find that SOCS1 colocalizes with Gag along the microtubule network and promotes microtubule stability. SOCS1 also increases the amount of Gag associated with microtubules. Both nocodazole treatment and the expression of the microtubule-destabilizing protein, stathmin, inhibit the enhancement of HIV-1 particle production by SOCS1. SOCS1 facilitates Gag ubiquitination and the co-expression of a dominant-negative ubiquitin significantly inhibits the association of Gag with microtubules. We thus propose that the microtubule network plays a role in SOCS1-mediated HIV-1 Gag transport and virus particle formation.

Structured summary:
MINT-7014185: *Gag* (uniprotkb:P05888) and *SOCS1* (uniprotkb:O15524) *colocalize* (MI:0403) by *cosedimentation* (MI:0027)
MINT-7014239: *Cullin 2* (uniprotkb:Q13617) *physically interacts* (MI:0218) with *RelA* (uniprotkb:Q04206), *RBX1* (uniprotkb:P62877), *SOCS1* (uniprotkb:O15524), *elongin B* (uniprotkb:Q15369) and *elongin C* (uniprotkb:Q15370) by *pull-down* (MI:0096)
MINT-7014046: *gag* (uniprotkb:P05888), *SOCS1* (uniprotkb:O15524) and *tubulin alpha* (uniprotkb:Q13748) *colocalize* (MI:0403) by *fluorescence microscopy* (MI:0416)
MINT-7014269: *tubulin alpha* (uniprotkb:Q13748) *physically interacts* (MI:0218) with *Gag* (uniprotkb:P05888) by *anti tag coimmunoprecipitation* (MI:0007)
MINT-7014036: *tubulin alpha* (uniprotkb:Q13748) and *SOCS1* (uniprotkb:O15524) *colocalize* (MI:0403) by *fluorescence microscopy* (MI:0416)
MINT-7014201: *Cullin 2* (uniprotkb:Q13617) *physically interacts* (MI:0218) with *RBX1* (uniprotkb:P62877), *SOCS1* (uniprotkb:O15524), *elongin B* (uniprotkb:Q15369) and *elongin C* (uniprotkb:Q15370) by *pull-down* (MI:0096)
MINT-7014257: *Gag* (uniprotkb:P05888) *physically interacts* (MI:0218) with *Ubiquitin* (uniprotkb:P62988) by *anti tag coimmunoprecipitation* (MI:0007)
MINT-7014221: *Cullin 2* (uniprotkb:Q13617) *physically interacts* (MI:0218) with *Gag* (uniprotkb:P05888), *elongin C* (uniprotkb:Q15370), *elongin B* (uniprotkb:Q15369), *SOCS1* (uniprotkb:O15524) and *RBX1* (uniprotkb:P62877) by *pull-down* (MI:0096)

1. Introduction

The human immunodeficiency virus 1 (HIV-1) employs multi-step and multi-factorial processes for producing progeny viruses during infection [1,2]. Virus must utilize the intrinsic transport machinery of the infected host cells to enable the active transport

Abbreviations: HIV, human immunodeficiency virus; SOCS1, Suppressor of cytokine signaling 1; KIR, kinase inhibitory region; MTOC, microtubule organizing center; Ub, ubiquitin; VLP, virus-like particle

* Corresponding authors. Address: AIDS Research Center, National Institute of Infectious Diseases, 4-7-1 Gakuen, Musashimurayama, Tokyo 208-0011, Japan (A. Ryo). Fax: +81 42 563 6291.
E-mail addresses: aryo@nih.go.jp (A. Ryo), nyama@nih.go.jp (N. Yamamoto).

0014-5793/$36.00 © 2009 Federation of European Biochemical Societies. Published by Elsevier B.V. All rights reserved.
doi:10.1016/j.febslet.2009.03.041

of viral proteins [3,4]. Several recent studies have identified cellular factors that modulate HIV-1 Gag trafficking and localization. These include AP-3δ, POSH, HP68, GGA and Trim22 [5–9]. Moreover, phosphatidylinositol-(4,5)-bisphosphate (PIP2) has been shown to control the targeting of Gag to the plasma membrane [10]. These findings point to a critical role of host cell factors in Gag assembly and release, but the precise molecular functions of these factors and the specific timing of their roles in this process remain largely unknown.

We recently reported that the suppressor of cytokine signaling 1 (SOCS1) is an inducible host factor during HIV-1 infection and plays an important role in the intracellular trafficking of Gag to the plasma membrane, resulting in the efficient production of HIV-1 particles [11]. Moreover, we have further shown that the function of SOCS1 in Gag trafficking and HIV-1 particle production is not principally due to the suppression of interferon/cytokine signaling, but is mediated via its interaction with the HIV-1 Gag polyprotein [11]. Importantly, the targeted depletion of SOCS1 results in the mistargeting and degradation of Gag in lysosomes, leading to a significant decrease in virus particle production [11].

In our current study, we have utilized SOCS1 as a molecular tool to further reveal the molecular mechanisms underlying the intracellular transport of HIV-1 Gag during viral infection. We reveal from our findings that SOCS1 regulates the Gag trafficking process via the microtubule-dependent cellular machinery. Furthermore, we find that Gag is also regulated by a ubiquitin signaling pathway which is accompanied by Gag ubiquitination. These findings shed new light on the mechanisms involved in the intracellular transport of HIV-1 Gag and provide important clues for the design of future novel therapeutic interventions against AIDS and related disorders.

2. Materials and methods

2.1. Antibodies

Antibodies (Abs) and fluorescent reagents were obtained from the following sources: rabbit polyclonal anti-myc (A-14) and rabbit polyclonal anti-SOCS1 (H-93) Abs (Santa Cruz Biotechnology); rabbit polyclonal anti-SOCS1 (Zymed Laboratories); mouse monoclonal anti-FLAG (M2), anti-α-tubulin, anti-acetylated-α-tubulin and anti-γ-tubulin Abs (Sigma, St. Louis, MO); rabbit polyclonal anti-stathmin antibody (Calbiochem); mouse monoclonal anti-myc antibody (9B11, Cell Signaling Technology); mouse monoclonal anti-cytokeratin 7, cytokeratin 18, vimentin and HIV-p24 Ab (Dako Cytomation). Immunoblotting, immunoprecipitation and immunofluorescent analyses were performed as described previously [11].

2.2. Plasmids and sequences

Expression constructs for SOCS1 have been described previously [12]. HIV-1 Gag constructs have also been described previously [13]. Stathmin cDNA was amplified by RT-PCR from a human kidney cDNA library using the primers 5′-AGCAAG CTTGCCACCATGGCTTCTTCTGATATCCAGG-3′ and 5′-GACGGATCC GTCAGCTTCAGTCTCGTCAG-3′ and then subcloned into the pcDNA3.1 vector. pcDNA3.1-myc-ubiquitin and its mutants were generated by PCR as described previously [14]. The siRNA sequences were as follows: SOCS1-siRNA, GGCCAGAACCTT CCTCCTCTT; control-siRNA, TCGTATGTTGTGTGGAATT. All expression constructs were validated by sequencing.

2.3. Microtubule-associated protein spin-down assays

Microtubule-associated proteins were collected using a microtubule-associated protein spin-down assay kit (Cytoskeleton, BK029) according to the manufacturer's instructions. Briefly, 293T cells were lysed in 0.5 ml of PEM buffer (80 mM PIPES, pH 6.9, 0.3% Triton X-100, 1 mM EGTA, 1 mM GTP, GTP, 1 mM $MgCl_2$) supplemented with 1 mM phenylmethylsulfonyl fluoride, 5 μg/ml leupeptin, 2 μg/ml aprotinin, 1 mM sodium orthovanadate, and 5 mM NaF. Cell lysates were incubated with taxol-stabilized microtubules, followed by ultracentrifuge at 100000×*g* for 40 min at 25 °C.

2.4. Cell culture

The 293T, COS-1, COS-7, HeLa and HOS cell lines and mouse embryonic fibroblasts (MEFs) were cultured in DMEM supplemented with 10% FBS. SOCS1−/− MEF cells were cultured as described previously [12].

2.5. In vitro interaction analysis

The in vitro interaction between HIV-1 Gag and the SOCS1-E3 complex was analyzed as follows: ^{14}C-labeled recombinant proteins (SOCS1, elongin B/C, Rbx1, biotin labeled cullin 2, and HIV-1 Gag) were synthesized in a wheat germ cell-free system as described previously [15]. The synthesized proteins were subsequently incubated in 120 μl of reaction buffer (50 mM Tris–HCl, pH 7.6, 50 mM $MgCl_2$, 500 mM CH_3COOK, 0.1 mM DTT and 1 mg/ml BSA) and streptavidin magnetic beads (Promega, Madison, WI) at 23 °C for 1 h. The precipitated proteins were then washed three times with reaction buffer and subjected to autoradiography.

3. Results

3.1. SOCS1 aligns with microtubule forming fibrous structures

SOCS1 has been shown previously to localize at both the perinuclear region and the microtubule organizing center (MTOC) [16]. This finding indicated the possible involvement of the microtubule network in the regulation of Gag by SOCS1. We thus addressed whether the Gag transport system is in fact mediated by microtubule integrity and if SOCS1 enhances this process. Immunofluorescent analysis with α-tubulin antibodies revealed that endogenous SOCS1 forms punctate structures that align with the microtubule network (Fig. 1A). Importantly, these signals were completely abolished when the cells were stained with anti-SOCS1 antibodies that had been pre-absorbed with recombinant SOCS1 protein, confirming the specificity of this antibody (Fig. 1B). Parallel experiments revealed that SOCS1 does not colocalize with other cytoskeletal components such as actin or intermediate filaments (Fig. 1C).

3.2. SOCS1 promotes microtubule stability

Given our finding that SOCS1 can tightly associate with microtubules, we next addressed whether SOCS1 affects microtubule stability. Stabilized microtubules are frequently enriched in tubulin that has undergone post-translational modifications such as acetylation [17]. We found that the high expression of SOCS1 results in higher amounts of acetylated microtubules in three different cell lines when compared with control cells (Fig. 2A) and that this trend is dose-dependent in COS-7 cells (Fig. 2B). On the other hand, SOCS1−/− mouse embryonic fibroblasts (MEFs) exhibited lower levels of acetylated α-tubulin compared with wild-type MEFs (Fig. 2C). These results indicate that SOCS1 does indeed contribute to the stabilization of microtubules.

Mammalian cells usually possess a population of microtubules that are resistant to the depolymerization effects of microtubule disorganizing reagents. We thus addressed whether SOCS1 impacts

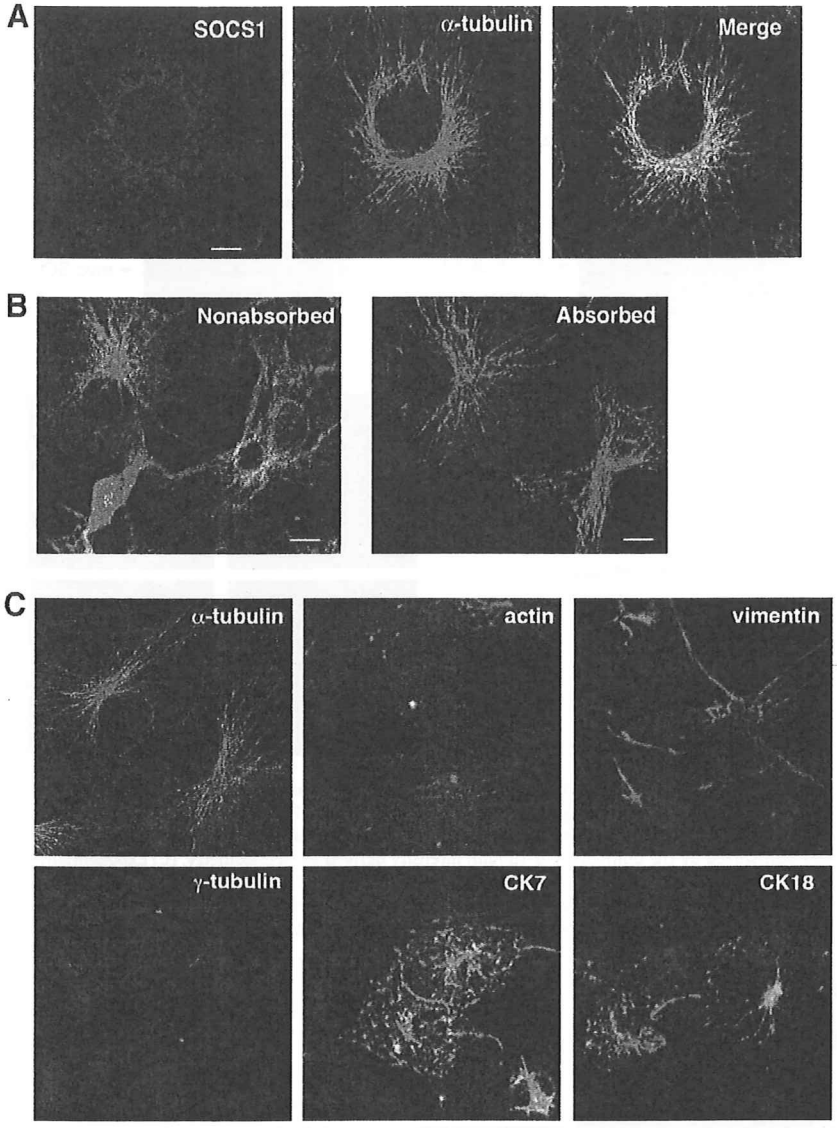

Fig. 1. SOCS1 colocalizes with microtubule forming fibrous structures. (A) COS-1 cells were fixed with 3% formaldehyde followed by 100% cold methanol, and then co-immunostained with polyclonal antibodies targeting SOCS1 (red) and monoclonal antibodies targeting α-tubulin (green). Cells were then analyzed by confocal microscopy. Scale bar, 10 μm. (B) COS-1 cells were immunostained with anti-α-tubulin monoclonal antibodies together with anti-SOCS1 polyclonal antibodies that had either been non-absorbed or pre-absorbed with GST-SOCS1 proteins. This was followed by confocal microscopy. Scale bar, 10 μm. (C) COS-1 cells were fixed with 3% formaldehyde followed by 100% cold methanol, then co-immunostained with polyclonal antibodies targeting SOCS1 (red) and monoclonal antibodies targeting various cytoskeletal components (green). Cells were then analyzed by confocal microscopy.

upon this property in this subpopulation of microtubules in COS-7 cells. The cells were transfected with either SOCS1 or control vector and then treated with 1 μM colchicine for 12 h to fully depolymerize the microtubules. Immunostaining with antibodies against acetylated α-tubulin showed that the SOCS1 expressing cells contained more polymerized microtubules compared with the control cells (Fig. 2D). These results indicate that SOCS1 might contribute to the microtubule stability required for Gag trafficking via this network.

3.3. SOCS1 enhances the association of HIV-1 Gag with microtubules

We next investigated the sub-cellular localization of HIV-1 Gag with SOCS1 and microtubules. COS-1 cells were transfected with Gag-GFP and after 24 h were fixed with 3% formaldehyde, followed by 100% cold methanol. The cells were then immunostained with anti-SOCS1 and anti-α-tubulin antibodies. Consistent with our earlier results, confocal microscopic analysis revealed that SOCS1 can form dotted filamentous structures in the cytoplasm along the microtubules, and that HIV-1 Gag colocalizes with these SOCS1 puncta (Fig. 3A).

To next determine whether cellular SOCS1 and Gag can together mechanically bind microtubules, and thus whether SOCS1 expression has any impact upon the interaction between Gag and microtubules, we performed microtubule pull-down analysis. 293T cells were transfected with either Gag-FLAG, myc-SOCS1, or a combination of these two plasmids, and the lysates from these transfected cells were subsequently incubated with taxol-stabilized microtubules and centrifuged to pellet the microtubule-associated proteins. The pellet fractions were then subjected to immunoblotting using either anti-myc or anti-FLAG antibodies. SOCS1 was found to be co-sedimented with microtubules irrespective of whether Gag had been co-transfected (Fig. 3B). The quantities of microtubule-bound Gag in the pellet fraction, however, were significantly increased when SOCS1 was co-transfected (Fig. 3B). These results together indicate that SOCS1 is itself a microtubule binding protein that may also mediate the interaction between HIV-1 Gag and microtubules.

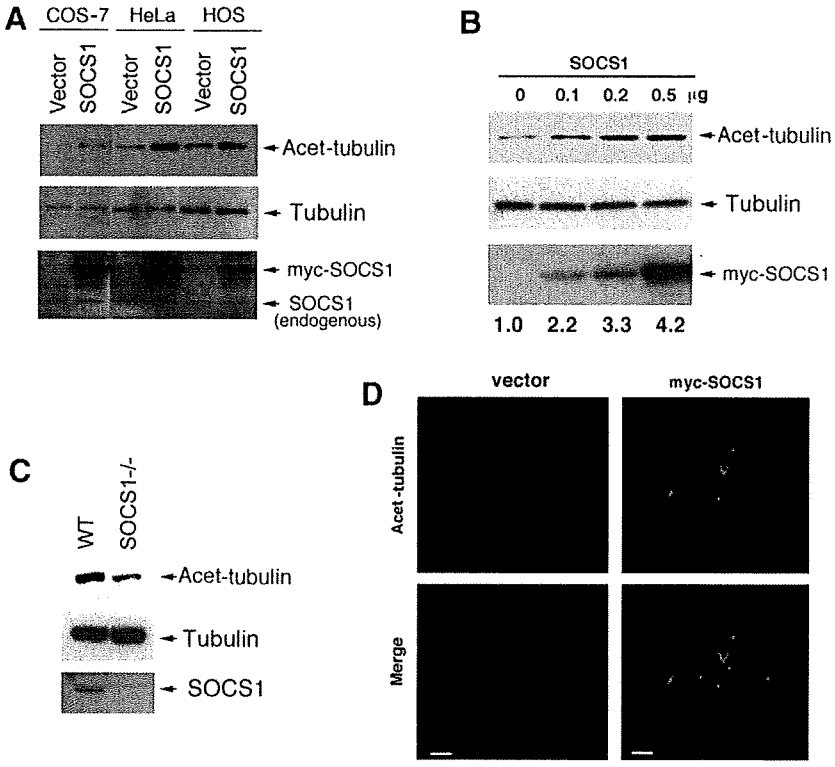

Fig. 2. SOCS1 enhances microtubule stability. (A) COS-7, HeLa or HOS cells were transfected with either empty vector or myc-SOCS1 for 48 h. Cell lysates were then subjected to immunoblotting analysis with antibodies against α-tubulin, acetylated α-tubulin or SOCS1. (B) COS-7 cells were transfected with various amounts of myc-SOCS1 as in (A). Cell lysates were then subjected to immunoblotting analysis with anti-α-tubulin, anti-acetylated-α-tubulin or anti-myc antibodies. Numerical values below the blots indicate acetylated α-tubulin signal intensities normalized by the unmodified α-tubulin intensity derived by densitometry. (C) Exponentially growing wild-type MEFs or SOCS1−/− MEFs were lysed and the cell lysates were immunoblotted with antibodies against α-tubulin, acetylated α -tubulin or SOCS1. (D) COS-7 cells were co-transfected with empty vector or myc-SOCS1, and then treated with colchicine (1 μM) for 12 h to depolymerize the microtubules. Cells were then fixed and immunostained with both anti-acetylated-α-tubulin (green) or anti-myc (red) antibodies and then stained with 4′,6-diamino-2-phenylindole (DAPI, blue), followed by confocal microscopy. Scale bar, 10 μm.

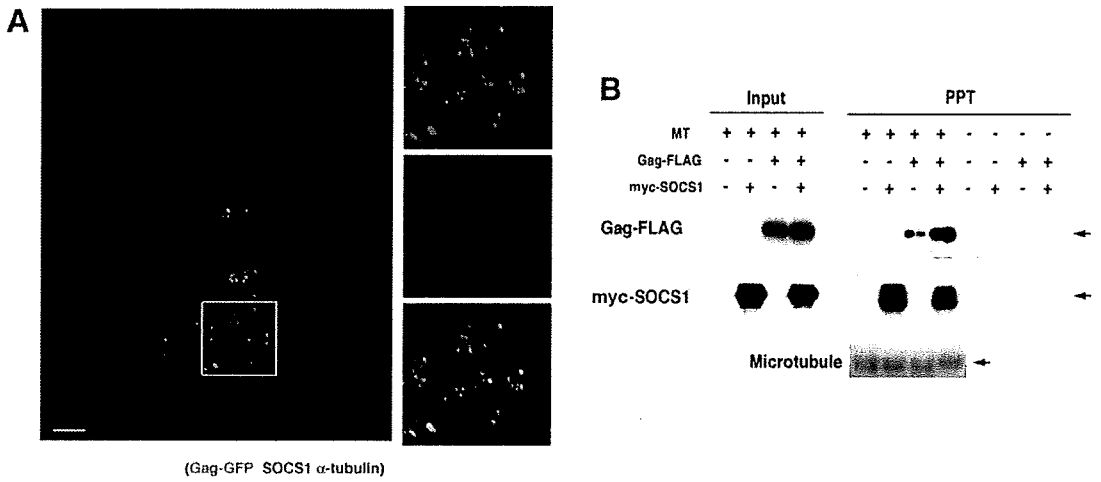

Fig. 3. SOCS1 enhances HIV-1 Gag associated with microtubules. (A) COS-1 cells transiently transfected with HIV-1 Gag-GFP were co-immunostained with antibodies targeting endogenous SOCS1 (red) and microtubules (α-tubulin, blue). The inset indicates the area shown at higher magnification in the right hand panels which reveal the colocalization of Gag-GFP with SOCS1 along the microtubules. Scale bar, 10 μm. (B) Cosedimentation of SOCS1 and HIV-1 Gag with polymerized microtubules. 293T cells were transfected with the indicated plasmids for 36 h. Cell lysates were then incubated with taxol-stabilized microtubules or control buffer and separated into precipitate (PPT) and supernatant fractions. Precipitate fractions were subjected to immunoblotting analysis with anti-myc or anti-FLAG antibodies.

3.4. Microtubule integrity is required for SOCS1 to function in HIV-1 particle formation

Our results shown above indicated that SOCS1 mediates the association of HIV-1 Gag with the microtubule networks. We next examined therefore whether SOCS1-mediated Gag trafficking, and the resultant HIV-1 particle production, are dependent upon an intact microtubule network. 293T cells were transfected with the HIV-1 molecular clone pNL4-3 and co-transfected with either empty vector alone or myc-SOCS1. After 24 h, the cells were washed with PBS and then cultured in the presence or absence of nocodazole for a further 6 h. Subsequent measurement of the p24 antigen levels in the cell supernatant by ELISA revealed nocodazole treatment significantly inhibited the enhancement of HIV-1 particle production in SOCS1-transfected cells more dramatically than in vector control transfected cells, and that this was

dose-dependent (Fig. 4A). Consistent with these results also, SOCS1 localization was observed to be significantly altered by nocodazole treatment, i.e. from a dotted filamentous structure along the microtubules to diffuse and larger aggregations in the cytoplasm (Fig. 4B). The use of trypan blue dye exclusion confirmed that cell viability was not affected by the nocodazole treatment (Fig. 4C).

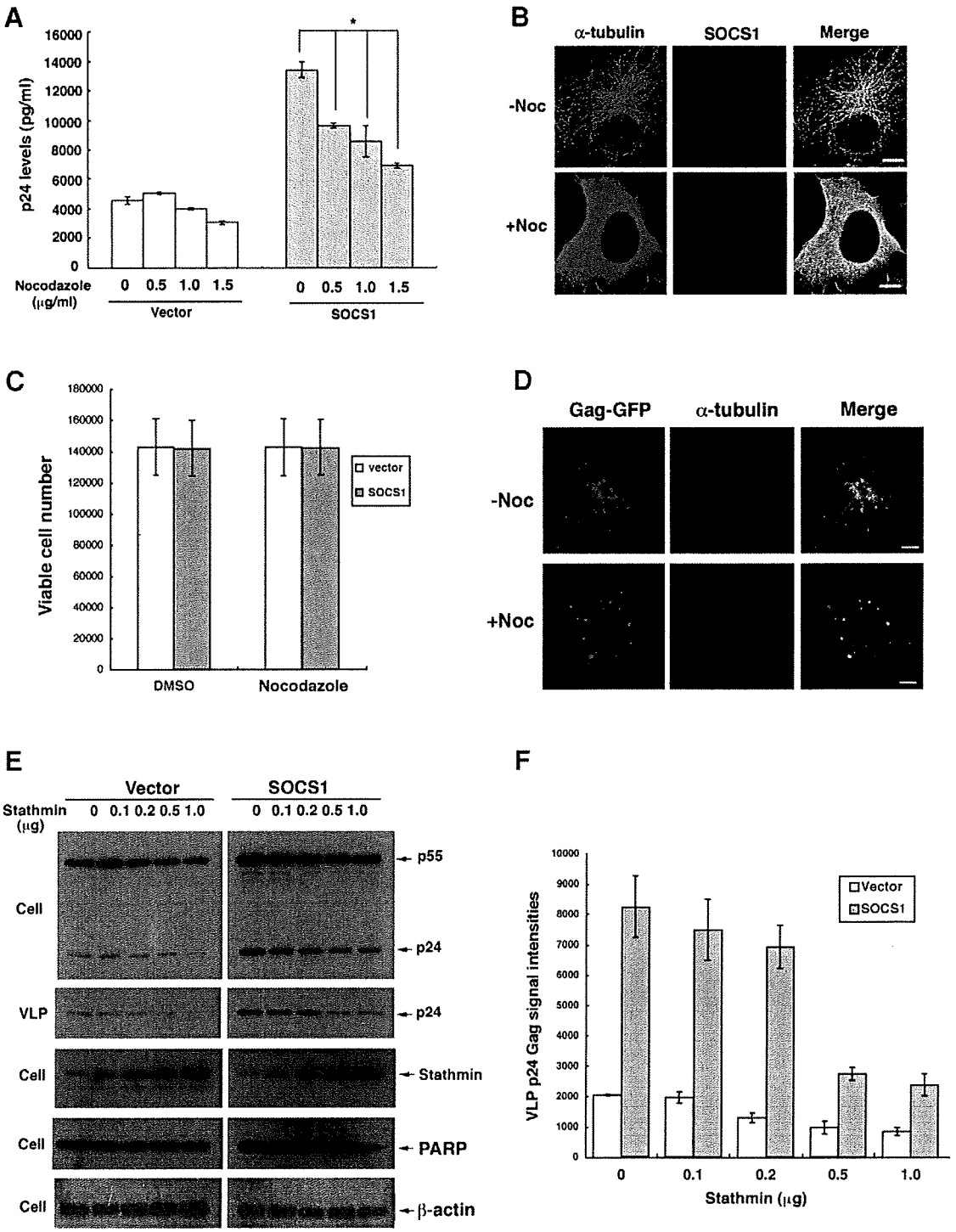

Fig. 4. Microtubule integrity is required for SOCS1 to function in HIV-1 particle formation. (A) 293T cells were transfected with pNL4-3, and co-transfected with either empty vector alone (Vector) or myc-SOCS1. After 24 h, cells were washed with PBS and then cultured with fresh media including the indicated concentrations of nocodazole for 6 h. Supernatant p24 antigen levels were measured by p24 ELISA . The data shown are the average ± S.D. of three independent experiments. $^{*}P \leqslant 0.05$, by the Student's *t*-test. (B and C) Mislocalization of SOCS1 in cells treated with nocodazole. COS-1 cells were treated with vehicle only or with nocodazole (2 μg/ml) for 6 h. Cells were then fixed and immunostained with both anti-SOCS1 (red) and anti-α-tubulin (green) antibodies, followed by confocal microscopy (B). Scale bar, 10 μm. The numbers of viable cells were calculated by trypan blue dye exclusion (C). (D) COS-1 cells transfected with Gag-GFP were treated with vehicle only or with nocodazole (2 μg/ml) for 6 h followed by immunostaining with anti-α-tubulin (red) antibody. Scale bar, 10 μm. (E and F) 293T cells were transfected with pNL4-3 and either vector or SOCS1, and co-transfected with various amounts of stathmin. At 36 h after transfection, cell lysate and supernatant virus-like particle (VLP) were processed for immunoblotting analysis with anti-p24, anti-PARP, anti-β-actin or anti-stathmin antibodies (E). VLP p24 Gag signal intensities, derived by densitometry, are shown in (F).

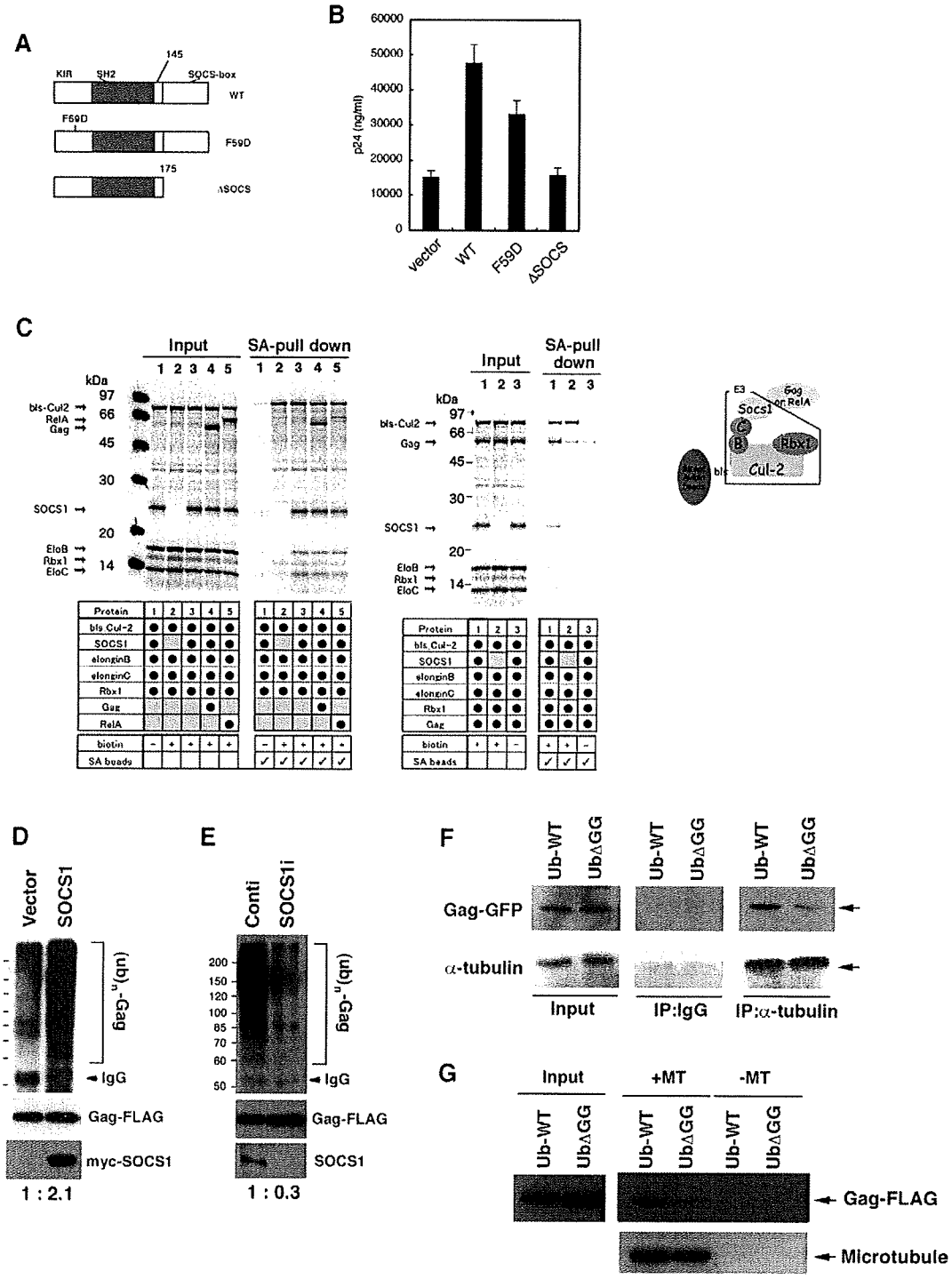

Fig. 5. SOCS1 enhances the ubiquitination of HIV-1 Gag and this affects the association of Gag with the microtubules. (A) Schematic represenation of SOCS1 mutants. (B) 293T cells were transfected with pNL4-3 and co-transfected with control vector, wild-type SOCS1 (WT), SOCS1-F59D mutant or ΔSOCS-box mutant. After 48 h, the p24 levels in the cell supernatants were measured by ELISA. (C) HIV-1 Gag associates with the ubiquitin ligase complex of SOCS1 in vitro. ^{14}C-labeled proteins (SOCS1, biotin labeled Cullin2, elongin B/C, Rbx1, HIV-1 Gag and RelA) were synthesized using a wheat germ cell-free system. Purified proteins were incubated in the indicated combinations for 1 h and subjected to co-purification with streptavidin magnetic beads. Captured proteins were then separated by SDS–PAGE followed by autoradiography. (D) 293T cells were co-transfected with Gag-FLAG, myc-tagged ubiquitin, and either empty vector (Vector) or SOCS1 expression construct. After 48 h, cells were lysed and denatured by boiling them in 1% SDS lysis buffer and diluted to RIPA buffer conditions, and Gag-FLAG proteins were immunoprecipitated (IP) with anti-FLAG antibody and processed for anti-myc immunoblotting to detect ubiquitinated Gag. Ubn, polyubiquitinated. Numerical values below blot indicates the relative levels of ubiquitinated Gag normalized by the amount of total Gag. (E) 293T cells were co-transfected with Gag-FLAG, myc-tagged ubiquitin, and either control-siRNA or SOCS1-siRNA. After 48 h, cell lysates were immunoprecipitated with anti-FLAG antibody and processed for anti-myc immunoblotting to detect ubiquitinated Gag. Ubn, polyubiquitinated. Numerical values below blot indicates the relative levels of ubiquitinated Gag normalized by the amount of total Gag. (F) 293T cells were transfected with Gag-GFP and SOCS1, and co-transfected with either myc-Ub-WT or myc-UbΔGG. After 24 h, cell lysates were harvested and subjected to immunoprecipitation analysis with anti-α-tubulin antibody or non-immunized mouse IgG (IgG) followed by immunoblotting analysis with the indicated antibodies. (G) 293T cells were transfected with Gag-FLAG and SOCS1, and co-transfected with either myc-Ub-WT or myc-UbΔGG. After 24 h, cell lysates were harvested and then incubated with taxol-stabilized microtubules (+MT) or control buffer (−MT), and separated into precipitate and supernatant fractions. Precipitate fractions were collected and then subjected to immunoblotting analysis with either anti-FLAG or anti-α-tubulin (microtubule) antibodies.